U.S. DEPARTMENT OF ENERGY | Office of Science

DOE/SC-ARM-TR-025

Solar Infrared Radiation Station (SIRS), Sky Radiation (SKYRAD), Ground Radiation (GNDRAD), and Broadband Radiometer Station (BRS) Instrument Handbook

A Andreas
A Habte
I Reda
M Dooraghi
M Kutchenreiter
M Sengupta

April 2018

ARM
CLIMATE RESEARCH FACILITY

DISCLAIMER

This report was prepared as an account of work sponsored by the U.S. Government. Neither the United States nor any agency thereof, nor any of their employees, makes any warranty, express or implied, or assumes any legal liability or responsibility for the accuracy, completeness, or usefulness of any information, apparatus, product, or process disclosed, or represents that its use would not infringe privately owned rights. Reference herein to any specific commercial product, process, or service by trade name, trademark, manufacturer, or otherwise, does not necessarily constitute or imply its endorsement, recommendation, or favoring by the U.S. Government or any agency thereof. The views and opinions of authors expressed herein do not necessarily state or reflect those of the U.S. Government or any agency thereof.

DOE/SC-ARM-TR-025

Solar Infrared Radiation Station (SIRS), Sky Radiation (SKYRAD), Ground Radiation (GNDRAD), and Broadband Radiometer Station (BRS) Instrument Handbook

A Andreas
M Dooraghi
A Habte
M Kutchenreiter
I Reda
M Sengupta
All at National Renewable Energy Laboratory

April 2018

Work supported by the U.S. Department of Energy,
Office of Science, Office of Biological and Environmental Research

Acronyms and Abbreviations

AC	alternating current
AIM	ARM Instrument Management (system)
AMF	ARM Mobile Facility
ARM	Atmospheric Radiation Measurement
ASTM	American Society for Testing and Materials
BIPM	International Bureau of Weights and Measures
BORCAL	Broadband Outdoor Radiometer CALibration
BRS	broadband radiometer station
BSRN	Baseline Surface Radiation Network (WMO)
CART	Cloud and Radiation Testbed
DC	direct current
DD	downwelling diffuse
DIR	downwelling infrared (atmospheric) irradiance
DOD	Data Object Design
DNI	Direct Normal Shortwave (Beam) Irradiance
DQAR	Data Quality Assessment Report
DQO	Data Quality Office
DQPR	Data Quality Problem Report
DQR	Data Quality Report
DS	downwelling shortwave (global)
EF	Extended Facilities
GMT	Greenwich Mean Time
GNDRAD	ground radiometers on stand for upwelling radiation
GUM	*Guide to Measurement Uncertainty*
IOP	Intensive Operational Period
IPC	International Pyrheliometer Comparisons
MCQ	Macquarie Island
MFRSR	multi-filter rotating shadowband radiometer
NPC	NREL Pyrheliometer Comparisons
NREL	National Renewable Energy Laboratory

NSA	North Slope of Alaska
OMIS	Operations Management Information System
OSS	Operations Status System
PNNL	Pacific Northwest National Laboratory
PRP	portable radiometer package
PSP	precision spectral pyranometer
QC	quality control
QME	Quality Measurement Experiment
RCF	Radiometer Calibration Facility
SGP	Southern Great Plains
SI	Système International d'unités
SIROS	solar and infrared radiation observation station
SIRS	solar infrared radiation station
SKYRAD	sky radiometers on stand for downwelling radiation
SRRL	Solar Radiation Research Laboratory
TWP	Tropical Western Pacific
UIR	upwelling infrared (terrestrial) irradiance
US	upwelling shortwave (reflected) irradiance
UTC	Coordinated Universal Time
VAP	value-added product
WISG	Interim World Infrared Standard Group
WMO	World Meteorological Organization
WRC	World Radiation Center
WRR	World Radiometric Reference

Contents

Figures

Tables

1.0 General Overview

The solar infrared radiation station (SIRS), ground radiometers on stand for upwelling radiation (GNDRAD), and sky radiometers on stand for downwelling radiation (SKYRAD) provide continuous measurements of broadband shortwave (solar) and longwave (atmospheric or infrared) irradiances for downwelling and upwelling components. The following six irradiance measurements are collected from a network of stations to help determine the total radiative flux exchange at each of the primary U.S. Department of Energy (DOE) Atmospheric Radiation Measurement (ARM) field research sites—(Southern Great Plains [SGP], North Slope of Alaska [NSA)]and Eastern North Atlantic [ENA])—as well as the ARM mobile facilities (AMF):

- Direct normal shortwave (solar beam)
- Diffuse horizontal shortwave (sky)
- Global horizontal shortwave (total hemispheric)
- Upwelling shortwave (reflected)
- Downwelling longwave (atmospheric infrared)
- Upwelling longwave (surface infrared).

Note: The SKYRAD and GNDRAD instruments used in the Eastern North Atlantic (ENA), North Slope of Alaska (NSA), and ARM Mobile Facility (AMF) sites are identical to those used by SIRS. The difference is that two data loggers are used, called SKYRAD and GNDRAD, to provide the downwelling and upwelling irradiance measurements, respectively. Additionally, the SKYRAD system has a redundant instrument measuring downwelling longwave radiation.

Commercially available, thermopile-based radiometers and supporting equipment (i.e., solar tracker, radiometer ventilator, and data acquisition system) comprise each SIRS installation as shown in Figure 1. An equipment summary is provided in Table 1.

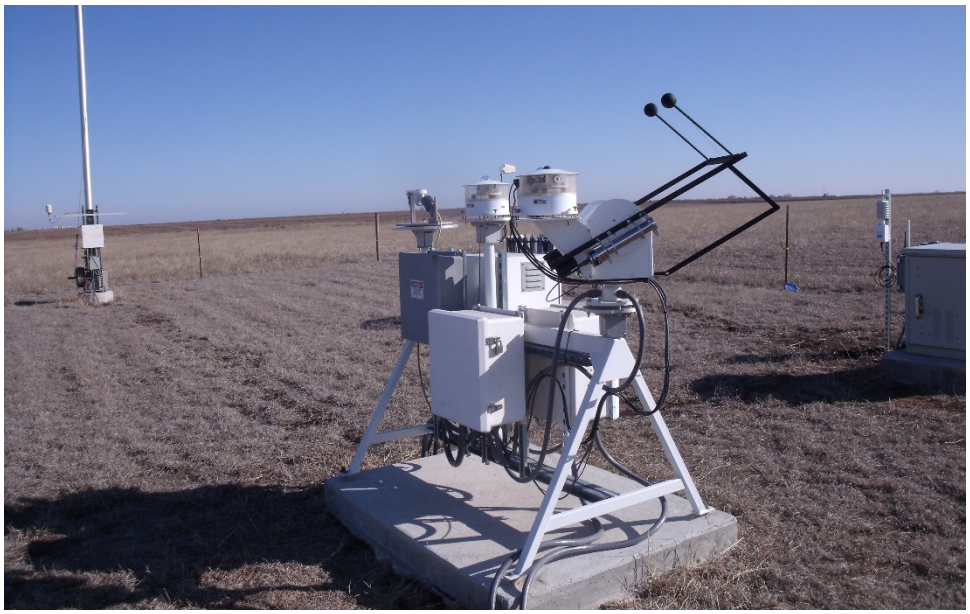

Figure 1. SIRS radiometers for downwelling irradiance measurements.

Table 1. Equipment summary.

Measurement	Radiometer Type[1]	Model[2]	Supporting Equipment
Direct Normal	Pyrheliometer	Normal Incidence Pyrheliometer (NIP)	Kipp & Zonen Model 2-AP automatic solar tracker
Diffuse Horizontal	Pyranometer	Precision Spectral Pyranometer (PSP) [Replaced by Model 8-48 (Black & White) after Feb 2000]	Kipp & Zonen Model 2-AP automatic solar tracker and Eppley Model V1 ventilator
Global Horizontal	Pyranometer	Precision Spectral Pyranometer (PSP)	Eppley Model V1 ventilator
Upwelling Shortwave	Pyranometer	Precision Spectral Pyranometer (PSP)	Custom stainless steel sun shade for inverted radiometer case and 10 m tower[3]
Downwelling Longwave (Shaded)	Pyrgeometer	Precision Infrared Radiometer (PIR)	Kipp & Zonen Model 2-AP automatic solar tracker and Eppley Model V1 ventilator
Upwelling Longwave	Pyrgeometer	Precision Infrared Radiometer (PIR)	Custom stainless steel sun shade for inverted radiometer case and 10 m tower[3]

Notes:
1. All radiometers manufactured by The Eppley Laboratory, Inc., Newport, Rhode Island, USA.
2. Shortwave (solar) radiometer spectral responses are 295 nm-3000 nm and longwave (infrared) radiometer spectral responses are 3.5 µm–50 µm.
3. Some AMF stations operate upwelling instruments on shorter towers.

2.0 Contacts

2.1 Mentors

Manajit Sengupta (Instrument Mentor) National Renewable Energy Laboratory Phone: 303-275-3706 Fax: 303-630-2401 Manajit.Sengupta@NREL.gov	Mark Kutchenreiter (Associate) National Renewable Energy Laboratory Phone: 303-384-7900 Fax: 303-384-6391 Mark.Kutchenreiter@nrel.gov
Mike Dooraghi (Associate) National Renewable Energy Laboratory Phone: 303-384-6329 Fax: 303-384-6391 Mike.dooraghi@nrel.gov	Aron Habte (Associate) National Renewable Energy Laboratory Phone: 303-384-6389 Fax: 303-384-6391 Aron.Habte@nrel.gov

2.2 Instrument Developers

The Eppley Laboratory, Inc. 12 Sheffield Avenue Newport, Rhode Island 02840 Phone: 401-847-1020 http://www.eppleylab.com	Kipp & Zonen, Delft BV 125 Wilbur Place Bohemia, New York 11716 Phone: 631-589-2065 ext 24 http://www.kippzonen.com

3.0 Station Deployment Locations and History

During the summer of 2014, there were a total of seven SKYRAD/GNDRAD sites, 1 broadband radiometer station (BRS) site, and 16 SIRS active sites in the ARM network, which comprises both fixed observatories and ARM mobile facilities (AMFs).

3.1 SIRS

As of April 2016, there were 10 operational SIRS sites in the network of SGP Central and Extended Facilities as summarized in Table 2 and shown in Figure 3. The SIRS radiometers are the same as those originally used by the solar and infrared radiation observation station (SIROS) instrument suite to measure the identical irradiance components as SIRS. The SIROS instruments included the multifilter rotating shadowband radiometer (MFRSR) and shared the data acquisition system. The SIRS offered data acquisition improvements that increased data recovery and eliminated the need for in-line amplifiers on each broadband radiometer. A change in the diffuse instrument was made in 2001 (see section 5.3.3.

Table 2. SIRS locations in the SGP Extended Facilities (EF), C1, and BRS.

OK Site	Elevation (m)	Lat., Long.	SIRS Operational Date[1]	Decommission Date
Ashton, KS: E-9	386	37.133, -97.266	2/6/98	--
Byron, OK: E-11	360	36.881, -98.285	8/20/97	--
Coldwater, KS: E-8	664	37.333, -99.309	8/19/97	10/28/2010
Cordell, OK: E-22	465	35.354, -98.977	11/24/97	12/1/2010
Cyril, OK: E-24	409	34.883, 98.205	11/25/97	11/24/2010
Earlsboro, OK: E-27	300	35.269, 96.740	5/02/02[2]	1/20/2010
Elk Falls, KS E-7	283	37.383, -96.180	10/31/97	11/14/2011
El Reno, OK: E-19	421	35.557, -98.017	6/16/98	5/25/2011
Halstead, KS E-5	440	38.114, -97.513	11/6/97	11/2/2010
Hillsboro, KS E-2	447	38.305, -97.301	11/6/97	10/21/2010
Lamont, OK: E-13	318	36.605, -97.485	8/25/97	--
Larned, KS: E-1	632	38.202, -99.316	11/20/97	10/15/2010
LeRoy, KS: E-3	338	38.201, -95.597	11/4/97	10/28/2010
Meeker, OK: E-20	309	35.564, -96.988	2/11/98	12/17/2009
Morris, OK: E-18	217	35.687, -95.856	9/30/97	11/17/2010
Okmulgee, OK: E-21	240	35.615, -96.065	7/22/99	--
Pawhuska, OK: E-12	331	36.841, -96.427	10/29/97	--
Plevna, KS: E-4	513	37.953, -98.329	11/7/97	9/27/2011
Ringwood, OK: E-15	418	36.431, -98.284	8/23/97	--
Seminole, OK: E-25	277	35.245, -96.736	10/01/97	4/8/2002
Anthony, KS: E-31	412	37.151, -98.362	09/16/11	--
Medford, OK: E-32	328	36.819, -97.820	08/25/11	--
Newkirk, OK: E-33	357	36.926, -97.081	08/16/11	--
Maple City, KS: E-34	417	37.069, -96.760	08/26/11	--
Tryon, OK: E-35	294	35.862, -97.069	09/01/11	--
Marshall, OK: E-36	340	36.117, -97.511	08/24/11	--
Waukomis, OK: E-37	379	36.311, -97.927	08/30/11	--
Omega, OK: E-38	367	35.880, -98.173	08/19/11	--
Towanda, KS: E-6	409	37.842, -97.020	11/05/97	10/18/2011
Tyro, KS: E-10	248	37.068, -95.788	10/30/97	10/19/2011
Vici, OK: E-16	602	36.061, -99.134	8/21/97	11/15/2011
Lamont, OK: C1	318	36.605, -97.485	1/15/97[3]	--
Lamont, OK: BRS	318	36.605, -97.485	3/5/2001[4]	--
Morrison, OK: E-39	279	36.374, -97.069	7/3/2015	--
Pawnee, OK: E-40	247	36.320, -96.765	10/7/2015	--
Peckham, OK: E-41	340	36.880, -97.086	4/13/2016	--

Notes:
1. Date of conversion from SIROS to SIRS data acquisition systems except as noted.
2. Earlsboro, Oklahoma site resumes data following system removal from Seminole site.
3. Date of installation for the "SIRS Testbed" at the Central Facility.
4. BRS consists of downwelling measurements only and is part of the World Meteorological Organization (WMO) Baseline Surface Radiation Network (BSRN) global network.

3.2 SKYRAD/GNDRAD

As of the April 3, 2016, there were four operational sites in the ARM network outside of the SGP facilities, including the North Slope of Alaska (NSA), Oliktok Point (OLI), Eastern North Atlantic (ENA), and Macquarie Island (MCQ) sites as summarized in Table 3. The SKYRAD/GNDRAD radiometers are the same as those used in the SIRS stations.

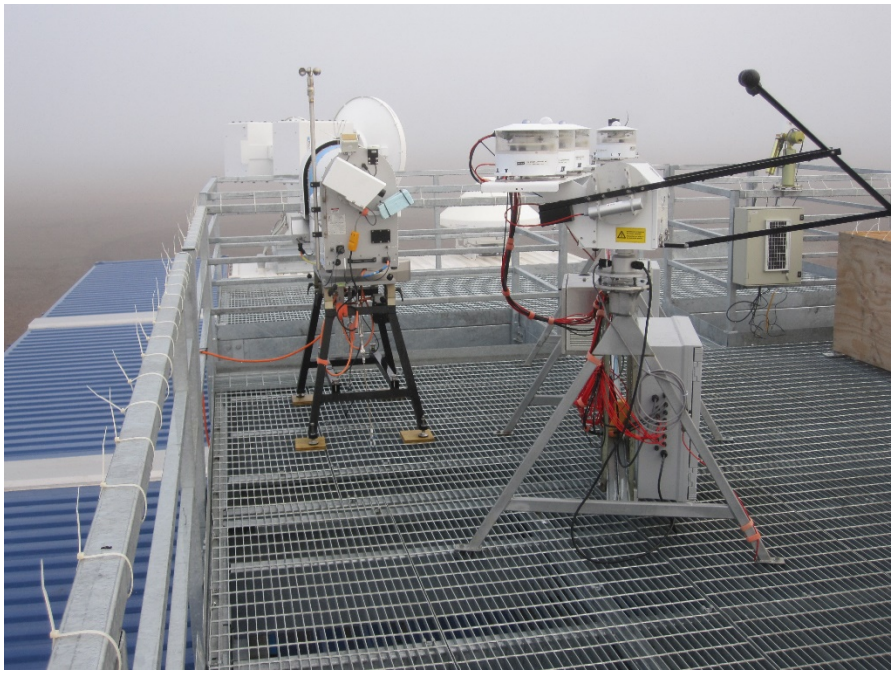

Figure 2. Typical SKYRAD installation at an ARM site.

Table 3. SKYRAD/GNDRAD locations at the NSA, Tropical Western Pacific (TWP), and AMF sites.[1]

Site	Operational Date	Decommission Date
Barrow, AK: NSA/C1	Feb 14, 1998	--
Azores, Portugal: ENA/C1	Sept 28, 2013	--
Atqusuk, AK: NSA/C2	Aug 21, 1999	Jan 17, 2011
Manus Island: TWP/C1	Oct 9, 1996	July 7, 2014
Nauru Island: TWP/C2	Oct 27, 1998	Aug 30, 2014
Darwin, Aus: TWP/C3	Mar 12, 2002	Jan 06, 2015
AMF1: Pt Reyes (PYE)	Feb 13, 2005	Sept 15, 2005
AMF1: Niger (NIA)	Nov 25, 2005	Jan 7, 2007
AMF1: Black Forest (FKB)	Mar 14, 2007	Jan 1, 2008
AMF1: China (HFE)	May 15, 2008	Dec 28, 2008
AMF1: Azores (GRW)	Apr 15, 2009	Jan 6, 2001
AMF1: India (PGH)	Jun 4, 2011	Mar 27, 2012

Site	Operational Date	Decommission Date
AMF1:Cape Cod (PVC)	Jun 05, 2012	Jul 9, 2013
AMF1: Manacapuru (MAO)	Dec 20, 2013	Dec 21, 2015
AMF1: Ascension Island (LASIC)	May 02, 2016	Nov 01, 2017
AMF1: Macquarie Island (MCQ)	Apr 03, 2016	--
AMF2: Steamboat Springs (SBS)	Sep 22, 2010	May 02, 2011
AMF2: Maldives (GAN)	Sep 23, 2011	Feb 09, 2012
AMF2: Long Beach (MAG)[2]	Oct 01, 2012	Sep 30, 2013
AMF2: Finland (TMP)	Jan 16, 2014	Sep 13, 2014
AMF2: McMurdo (AWARE)	Nov 16, 2015	Dec 29, 2016
AMF2: Antarctic Ice Sheet (AWARE)	Dec 04, 2015	Jan 19, 2016
AMF3: Oliktok Point (OLI)	Sept 25, 2013	--

Notes:
1. Visit the ARM IOP web page link for dates, location, and other specifics (http://www.arm.gov/campaigns).
2. Portable Radiometer Package (shipboard PRP).

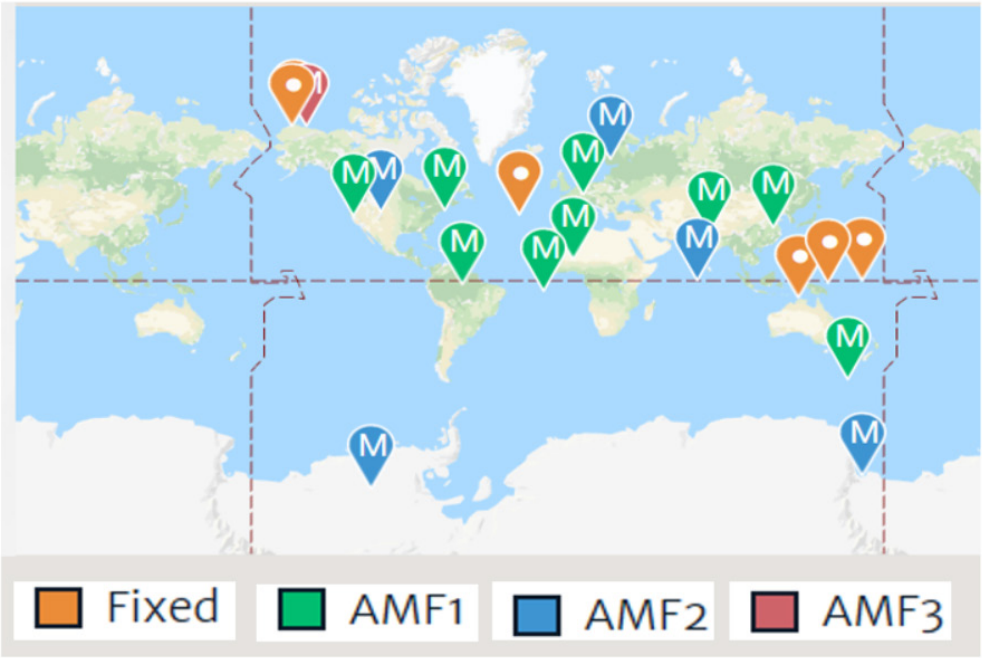

Figure 3. SKYRAD/GMDRAD locations at the NSA, TWP, and AMF sites.

3.3 BRS

The broadband radiometer station (BRS) is located at the ARM SGP site Central Facility, near the solar and infrared radiation station (SIRS) C1 station. The BRS station collection of radiometers provides

continuous measurements of broadband shortwave (solar) and longwave (infrared) irradiances for downwelling components. These 1-minute data are collected to help determine the radiative energy exchange. The BRS station is similar in design to the ARM SKYRAD stations and is operated by ARM in association with the Baseline Surface Radiation Network (BSRN, http://bsrn.awi.de). Note that there are no upwelling measurements at this station. Like C1 and E13, this station is cleaned daily, as opposed to the bi-weekly cleaning at the Extended Facility sites.

Figure 4. Tracker-mounted PIR, 8-48, and NIP radiometers at the SGP BRS site.

Figure 5. Single global PSP radiometer on pedestal at the SGP BRS site.

Table 4. BRS dates SGP facilities.[1]

Site	Operational Date	Decommission Date
Central Facility Lamont, OK: (SGP C1/BRS)	Mar 05, 2001	--
Notes: 1. Visit the ARM IOP Web page link for dates and location and other specifics (http://www.arm.gov/campaigns)		

4.0 Near-Real-Time Data Plots

Daily Plots, from ARM Data Quality Diagnostic Plot Browser (http://plot.dmf.arm.gov/plotbrowser/)

SGP Site Scientist Data Quality Assessment from ARM Data Quality Health & Status Explorer (http://dq.arm.gov/)

5.0 Data Description and Examples

Typical SIRS Data Time Series Plots

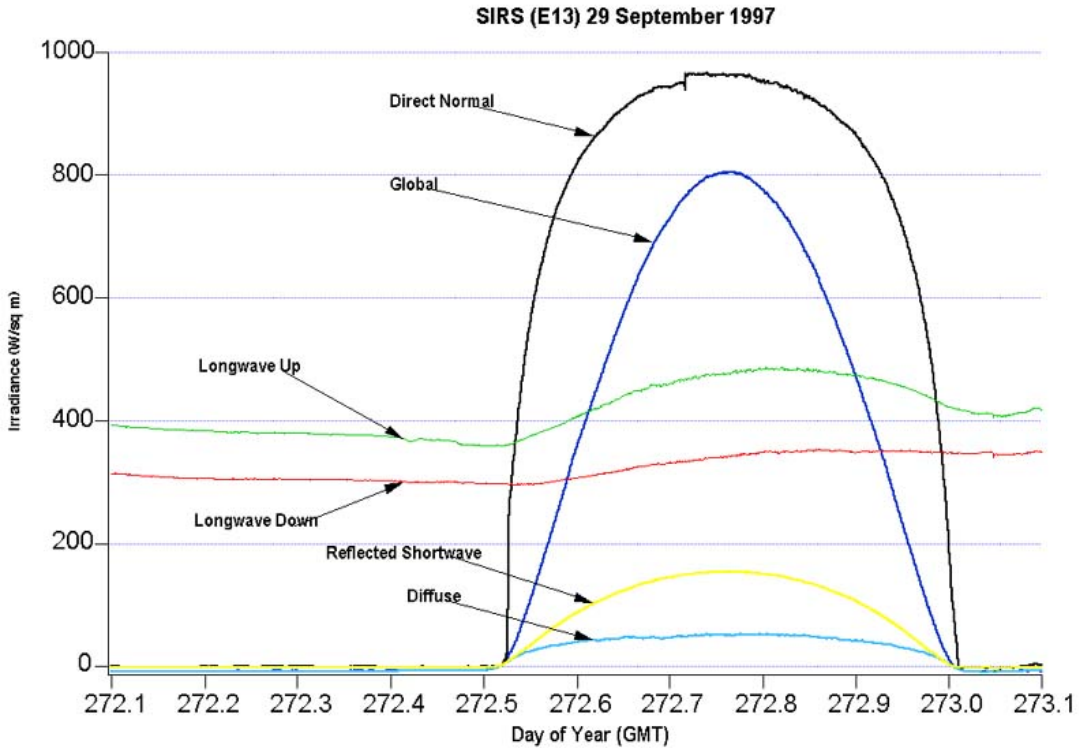

Figure 6. Clear-sky time-series plot of 1-minute SIRS measurements.

Data in Figure 6 are typical of the clear-sky conditions at the SGP during the fall. Near solar noon, when the sun is highest in the sky and there is the least amount of atmosphere in the photons' path to the surface, the direct normal shortwave (beam) irradiance approaches 1000 Wm^{-2}, the global (total hemispheric) irradiance nears 800 Wm^{-2}, the diffuse (sky) irradiance remains nearly constant at about 50 Wm^{-2}, and the reflected shortwave reaches a peak of 155 Wm^{-2} (for a surface albedo, global/reflected, of about 19%, which is typical for a vegetated surface). Heating of the surface and the atmosphere is evident from the increasing longwave (infrared) irradiance measurements. The peak longwave irradiances occur after solar noon, demonstrating the "thermal lag" of the earth-atmosphere system response to solar heating. The peak upwelling longwave irradiance on this day was 488 Wm^{-2} at 19:41 GMT (1:41 PM local standard time). The peak downwelling (atmospheric) longwave irradiance was 355 Wm^{-2} at about the same time, producing a net radiation of 133 Wm^{-2}. The effect of cleaning the pyrheliometer window is evident from the change in direct normal irradiance prior to local solar noon. Maintenance records show the pyrheliometer window was dry, but had light dust removed from the surface at 17:10 GMT. Comparing the direct normal data before and after the cleaning, 947.81 Wm^{-2} and 963.25 Wm^{-2} respectively, suggests a decreased irradiance measurement of 1.6% due to the window contamination.

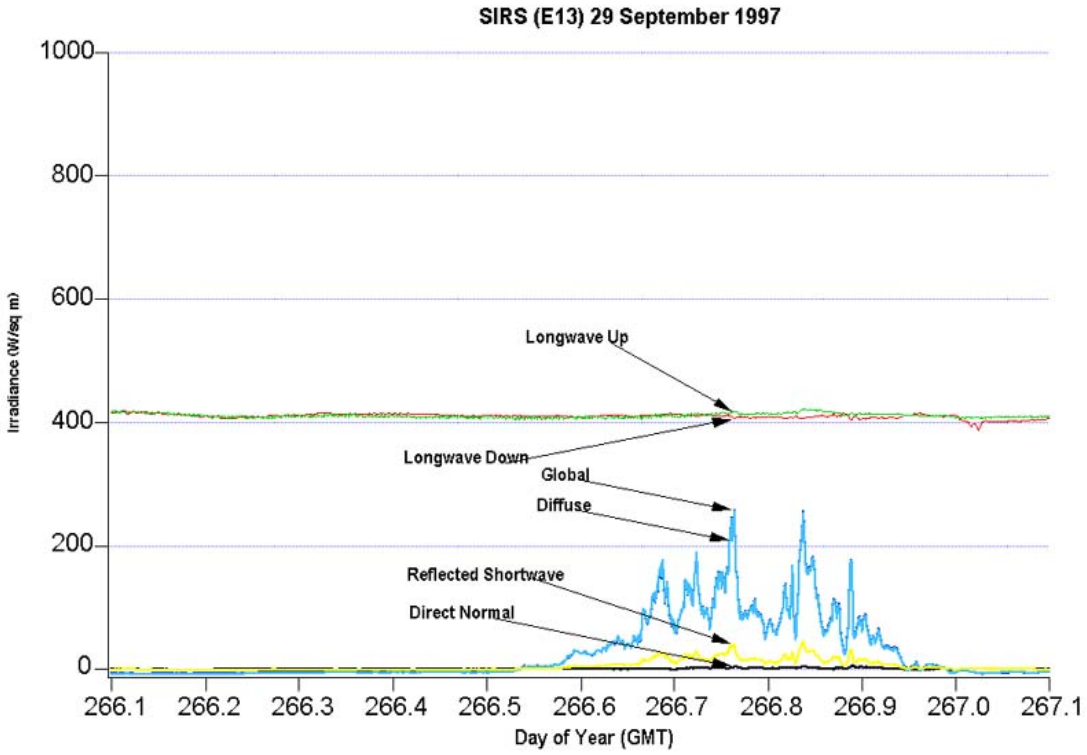

Figure 7. Overcast-sky time-series plot of 1-minute SIRS measurements.

Data in Figure 7 are typical of cloudy sky conditions at the SGP during the fall. With completely overcast conditions, the direct normal shortwave (beam) irradiance remains near zero all day. Variable cloud thickness during the day allow the global (total hemispheric) and the diffuse (sky) irradiance to peak at about 256 Wm^{-2} at 18:20 GMT and a few hours later. The reflected shortwave reaches a peak of 45 Wm^{-2} (albedo of about 18%). The exchange of infrared radiation is nearly constant under these conditions, suggesting low clouds. The two SIRS pyrgeometers indicate 415 W^{-2} of longwave irradiance was consistently measured at the Central Facility on 23 September, 1997.

5.1 Data File Contents

5.1.1 Primary Variables and Expected Uncertainty

The following *broadband* irradiance measurements are available from the SIRS/SKYRAD and GDNRAD platforms and are summarized in Table 4:

Downwelling Shortwave (0.3 to 3.0 micrometers)

1. Direct Normal (beam) irradiance measured by a pyrheliometer with a 5.7 degree field of view.
2. Diffuse Horizontal (sky) irradiance measured by a shaded and ventilated pyranometer with a hemispherical field of view, but blocked from the direct normal irradiance by a tracking ball.
3. Total Hemispheric (global) irradiance measured by an unshaded and ventilated pyranometer.

Downwelling Longwave (3.5to 50 micrometers)

4. Total Hemispheric (atmospheric) irradiance measured by a shaded and ventilated pyrgeometer with a hemispheric field of view.

Upwelling Shortwave (0.3 to 3.0 micrometers)

5. Reflected solar irradiance measured by an inverted pyranometer with a hemispheric field of view.

Upwelling Longwave (3.5 to 50 micrometers)

6. Irradiance measured by an inverted pyrgeometer with a hemispheric field of view.

Table 5. Primary variables.

Variable Name	Quantity Measured	Unit
short_direct_normal	Direct normal (beam) solar irradiance	Wm^{-2}
down_short_diffuse_hemisp	Diffuse horizontal (sky) solar irradiance	Wm^{-2}
down_short_hemisp	Total hemispheric (global) solar irradiance	Wm^{-2}
down_long_hemisp_shaded	Total hemispheric (atmospheric) infrared irradiance	Wm^{-2}
up_short_hemisp	Reflected solar irradiance	Wm^{-2}
up_long_hemisp	Upwelling longwave irradiance	Wm^{-2}

5.1.2 Definition of Uncertainty

All measurements are approximations and are incomplete without a quantitative uncertainty estimate. The *Guide to Measurement Uncertainty (GUM)* of the International Bureau of Weights and Measures (BIPM, 1995) is the accepted international guide for performing a measurement uncertainty analysis. The *GUM* defines *Type A* uncertainty values as derived from statistical methods, and *Type B* sources as evaluated by "other means", such as scientific judgment, experience, specifications, comparisons, or calibration data.

Each element of a measurement system contributes to the limits of uncertainty. When a result, R, is functionally dependent upon several variables, x_i, then the familiar propagation of error formula is used,

$$U_R^2 = \sum_i (\partial_{X_i} R \cdot e_{X_i})^2 \qquad \text{[eq. 1]}$$

where,

U = uncertainty in the resultant,
e_{xi} = estimated uncertainty in variable x_i, and
$\partial_{xi}R$ = partial derivative of the response R with respect to variable x_i, (also called the sensitivity function for variable x_i).

Radiometer measurement uncertainty analyses have historically treated sources of uncertainty in terms of "random" and "bias" components (Myers, et al., 1989). Total uncertainty (U) was computed from:

$$U^2 = \Sigma\,(\text{Bias})^2 + \Sigma\,(2*\text{Random})^2 \qquad \text{[eq. 2]}$$

A factor of two was applied to the "random" or statistical uncertainty component, because this component usually represented a standard deviation. One standard deviation of a normal or Gaussian distribution encompasses only 37% of the measured values and two standard deviations encompasses approximately 95% of the measured values. Thus, this method was considered to report uncertainty with a 95% "confidence interval." For example, the resulting uncertainty in the *calibration* of pyranometer responsivity and *field measurements* was ±2.4%, and ±5%, respectively.

The GUM replaces the factor of two with a "coverage factor", *k*, and determines the uncertainty from the following equation:

$$U^2 = \Sigma \text{ (Type B)}^2 + \Sigma \text{ (}k\text{* Type A)}^2$$

For small (n < 20) samples, from a Gaussian distribution of measurements, *k* may be selected from the student's t-distribution (Taylor and Kuyatt, 1993) and U is the "Expanded Uncertainty" where *k* is usually in the range of 2 to 3, for confidence intervals of 95% and 99%, respectively. The following estimates of measurement uncertainty follow the GUM approach.

Estimating radiometer measurement uncertainties is a topic of continuing research. Based on experiences with these and similar instruments for renewable energy applications, the following estimated measurement uncertainties conservatively apply to radiometric measurements (Table 5).

Table 6. Estimated measurement uncertainty of irradiance measurements.

Measurement	Abbreviation	Radiometer Model	Typical Responsivity (μV/Wm^{-2})	Calibration and Measurement Uncertainty
Direct Normal (beam)	DNI	NIP	8.0	±3.0% (>700Wm^{-2}) *
Diffuse Horizontal (sky)	DD	8-48	9.0	+ 4.0% to -(4% + 2 Wm^{-2}) *
Diffuse Horizontal (sky)	DD	PSP	8.0	+ 4.0% to -(4% + 20 Wm^{-2}) *
Downwelling Shortwave (global)	DS	PSP	9.0	±4.0% to –(4%+20 Wm^{-2}) Zenith < 80° *
Downwelling Longwave (atmospheric)	DIR	PIR	4.0	±(5.0% + 4 Wm^{-2}) **
Upwelling Shortwave (reflected)	US	PSP	9.0	±2.0% or 10 Wm^{-2} *
Upwelling Longwave (terrestrial)	UIR	PIR	4.0	±2.0 Wm^{-2} or 2 Wm^{-2} **

* WRR uncertainty
** WISG uncertainty
All uncertainties are estimated with respect to the Système International d'unités (SI) and represent optimal maintenance and installation. (Reda, et al., 2012, 2011)

5.1.3 Secondary/Underlying Variables

Table 7. Secondary variables.

Variable Name	Quantity Measured	Unit
short_direct_normal_std	Direct Normal (Beam) Solar Irradiance, Standard Deviation	Wm^{-2}
short_direct_normal_max	Direct Normal (Beam) Solar Irradiance Maxima	Wm^{-2}
short_direct_normal_min	Direct Normal (Beam) Solar Irradiance Minima	Wm^{-2}
down_short_diffuse_hemisp_std	Diffuse Horizontal (Sky) Solar Irradiance, Standard Deviation	Wm^{-2}
down_short_diffuse_hemisp_max	Diffuse Horizontal (Sky) Solar Irradiance Maxima	Wm^{-2}
down_short_diffuse_hemisp_min	Diffuse Horizontal (Sky) Solar Irradiance Minima	Wm^{-2}
down_short_hemisp_std	Total Hemispheric (Global) Solar Irradiance, Standard Deviation	Wm^{-2}
down_short_hemisp_max	Total Hemispheric (Global) Solar Irradiance Maxima	Wm^{-2}
down_short_hemisp_min	Total Hemispheric (Global) Solar Irradiance Minima	Wm^{-2}
down_long_hemisp_shaded_std	Total Hemispheric (Atmospheric) Infrared Irradiance, Standard Deviation	Wm^{-2}
down_long_hemisp_shaded_max	Total Hemispheric (Atmospheric) Infrared Irradiance Maxima	Wm^{-2}
down_long_hemisp_shaded_min	Total Hemispheric (Atmospheric) Infrared Irradiance Minima	Wm^{-2}
up_short_hemisp_std	Reflected Solar Irradiance, Standard Deviation	Wm^{-2}
up_short_hemisp_max	Reflected Solar Irradiance Maxima	Wm^{-2}
up_short_hemisp_min	Reflected Solar Irradiance Minima	Wm^{-2}
up_long_hemisp_std	Upwelling longwave irradiance, Standard Deviation	Wm^{-2}
up_long_hemisp_max	Upwelling longwave irradiance, Maxima	Wm^{-2}
up_long_hemisp_min	Upwelling longwave irradiance, Minima	Wm^{-2}
inst_up_long_dome_temp	Instantaneous Upwelling Pyrgeometer Dome Thermistor Temperature, Pyrgeometer	K
inst_up_long_case_temp	Instantaneous Upwelling Pyrgeometer Case Thermistor Temperature, Pyrgeometer	K
inst_down_long_shaded_dome_temp	Instantaneous Downwelling Pyrgeometer Dome Thermistor Temperature, Shaded Pyrgeometer	K
inst_down_long_shaded_case_temp	Instantaneous Downwelling Pyrgeometer Case Thermistor Temperature, Shaded Pyrgeometer	K
up_long_netir	Upwelling Longwave Hemispheric Net Infrared	Wm^{-2}
down_long_netir	Downwelling Longwave Hemispheric Net Infrared	Wm^{-2}

5.1.4 Diagnostic Variables

The battery voltage is recorded at 1-minute intervals to confirm adequate electrical power was available to the Campbell Scientific, Inc. data logger. Nominally 13 VDC, an acceptable voltage range 10-16 VDC is required to assure proper operation (especially regulated excitation voltage need for thermistor measurements).

Lists of past and current primary, secondary, and diagnostic variables are contained within the Data Object Design (DOD) for each site's data ingest program as managed by the ARM Data Management Facility at Pacific Northwest National Laboratory (PNNL). The DODs for all SIRS/GNDRAD/SKYRAD can be viewed at (https://engineering.arm.gov/pcm/Main.html): select the datastreams tab and filter list by name "sirs", "skyrad" or "gndrad". Under each "Process Output Datastream Classes" is the history of the DODs for the selected datastream. In most cases the highest numerical DOD version is the most recent.

5.1.5 Data Quality Flags

Until early 2012, each 1-minute irradiance value was assigned a two-digit data quality flag based on the results of automated assessments developed by the National Renewable Energy Laboratory (NREL). This system was called SERI QC. When the SIRS ingest was ported to Linux in early 2012, the SERIQC system was replaced with a simplified max/min/delta QC flag system. Users are now directed to the QCRAD Value-Added Product (VAP) available for all SIRS, SKYRAD, GNDRAD, and BRS sites. Appendix 1 contains additional background and links for this product.

5.1.6 Dimension Variables

N/A

5.2 Annotated Examples of Instrument Failures and Proper Operation

5.2.1 Properly Operating Three-Component Shortwave Instruments

Variable precision spectral pyranometer (PSP) responsivity affects nearly any combination of shortwave instruments where a three-component calculation is performed. The derived minus the measured downwelling shortwave (DS) when plotted as a time series for a day will demonstrate a symmetric valley in the summer and a mountain in the winter. Figure 8 illustrates this relationship during proper operation. This characteristic is primarily due to the non-linear responsiveness of the PSP global horizontal instrument to solar zenith and azimuth position.

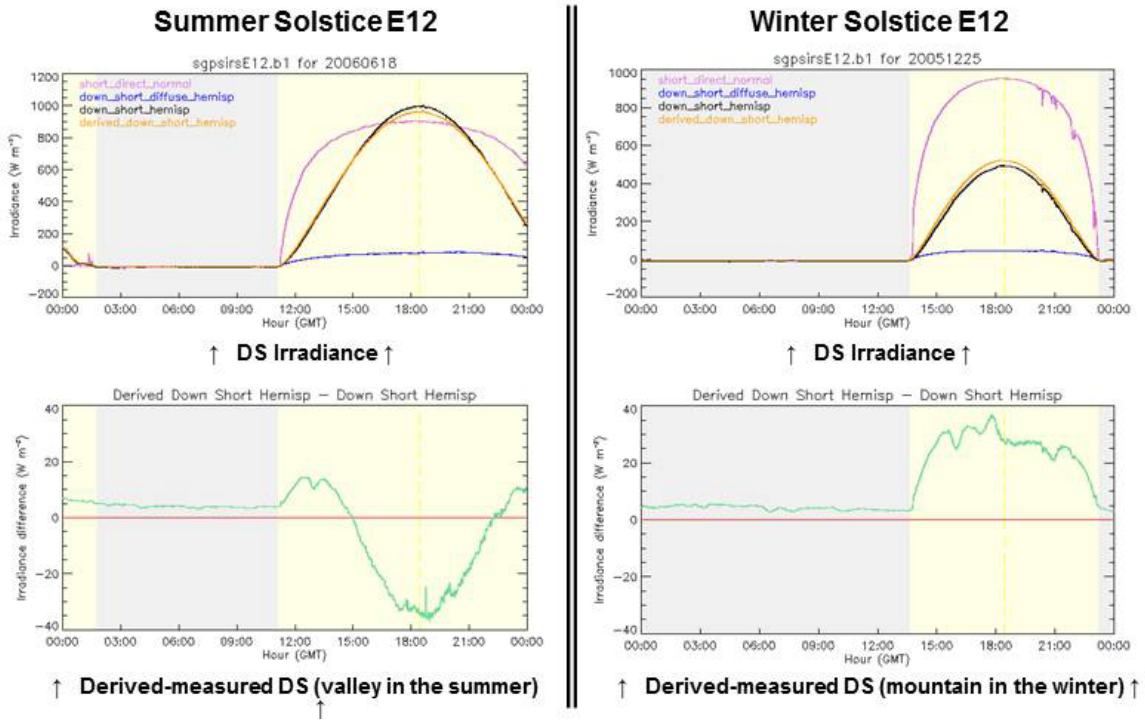

Figure 8. Properly operating three-component SW instruments.

5.2.2 Three-Component Mismatch

In Figure 9, the two upper graphs show that the difference between the measured and derived downwelling shortwave was as high as -80 Watts/m^2. In this instance, all shortwave instruments had been recently installed and the mentors questioned the larger difference in derived and measured downwelling shortwave that resulted after the instrument switch. The newly installed instruments had little "installed" history and it was decided that all three instruments (global, diffuse, and direct) would be replaced. All shortwave instruments were replaced and the difference in derived and measured downwelling shortwave improved as seen in the lower two graphs.

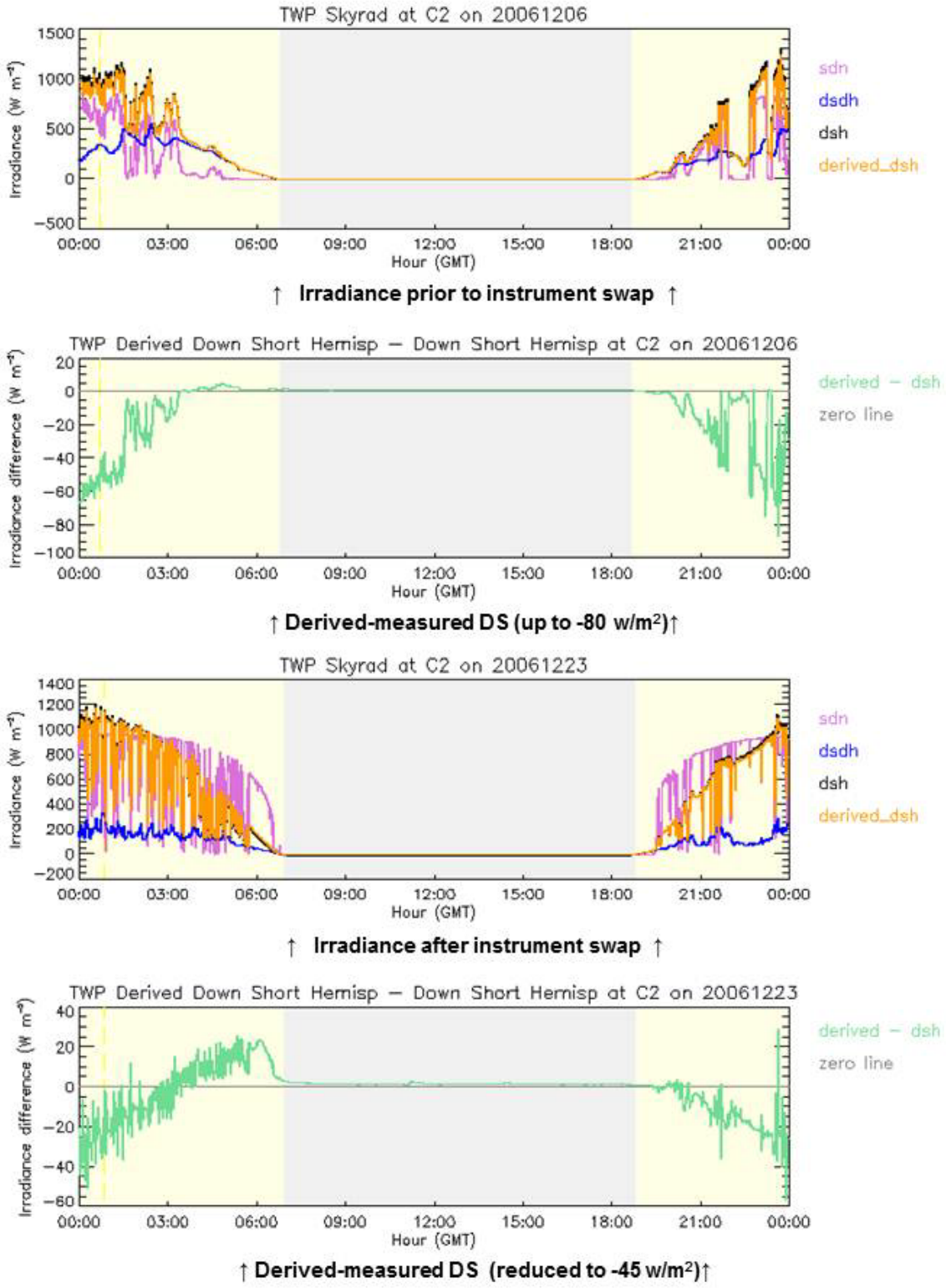

Figure 9. Three-component mismatch.

5.2.3 Infrared Measurement Deviation between IRT and PIR

Figure 10 illustrates a large difference between the measured longwave from the pyrgeometer versus the calculated longwave from the infrared thermometer. This indicates that one of the two devices is not operating correctly.

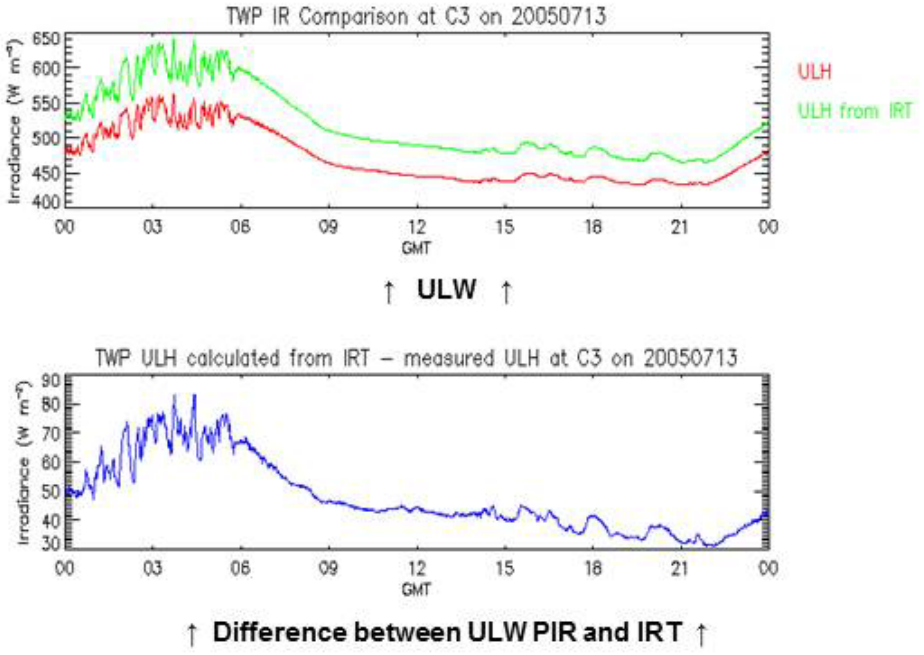

Figure 10. Infrared measurement deviation between IRT and PIR.

5.2.4 Asymmetry between Three-Component Instruments

Figure 11 illustrates asymmetry between the measured DS and the calculated DS. As mentioned in 5.2.1, the difference the measured and derived DS will form a symmetric valley in the summer and a mountain in the winter. The lower time series graph in Figure 11 illustrates two mountains with a valley in between as opposed to the expected single mountain or valley. This asymmetry can also be visually identified in the relationship between the direct and the global measurement in the irradiance time series. This is often caused by an unleveled PSP global horizontal instrument.

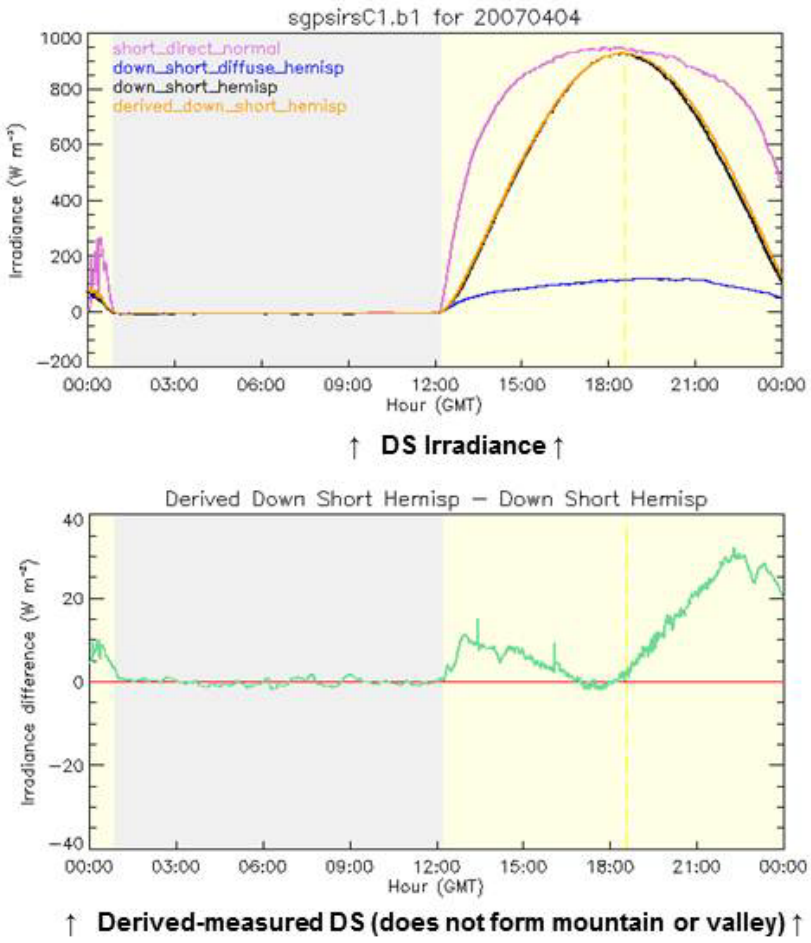

Figure 11. Asymmetry between three-component instruments.

5.2.5 Clogged Ventilator Fan

Figure 12 illustrates the noise that can be seen in the irradiance data when a ventilator is clogged. As seen in the upper graph, there is a lot of noise in the longwave measurement for the "shaded 1" instrument as compared to the "shaded 2" instrument. Once the ventilator was cleaned, the daytime gap between the two instruments and the noise in the signal from the instrument with the clogged filter were reduced.

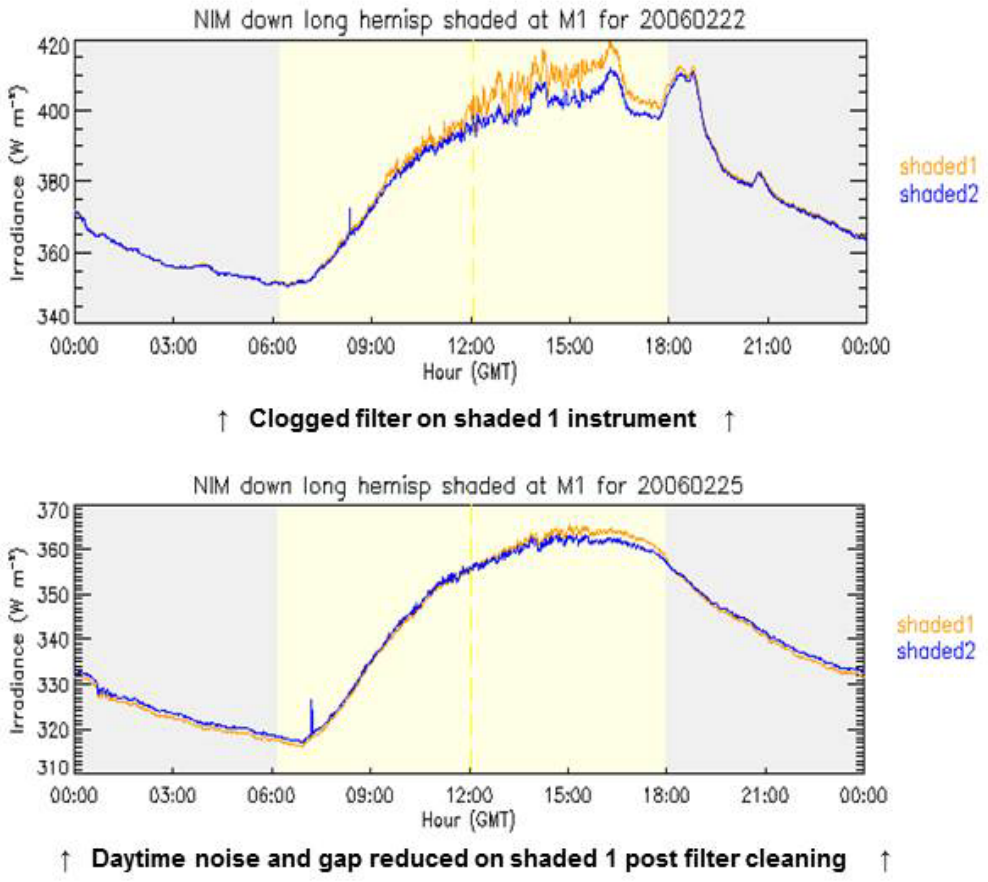

Figure 12. Clogged ventilator fan.

5.2.6 Dirty PSP Dome

Figure 13 illustrates a PSP with a dirty dome. The relationship between the measured and derived DS in the time series plot does not show the expected mountain or valley. Rather, there are sharp changes in this relationship throughout the day and an asymmetry can be seen in the global measurement. After the dome was cleaned, the time series displayed the expected valley for a summer measurement.

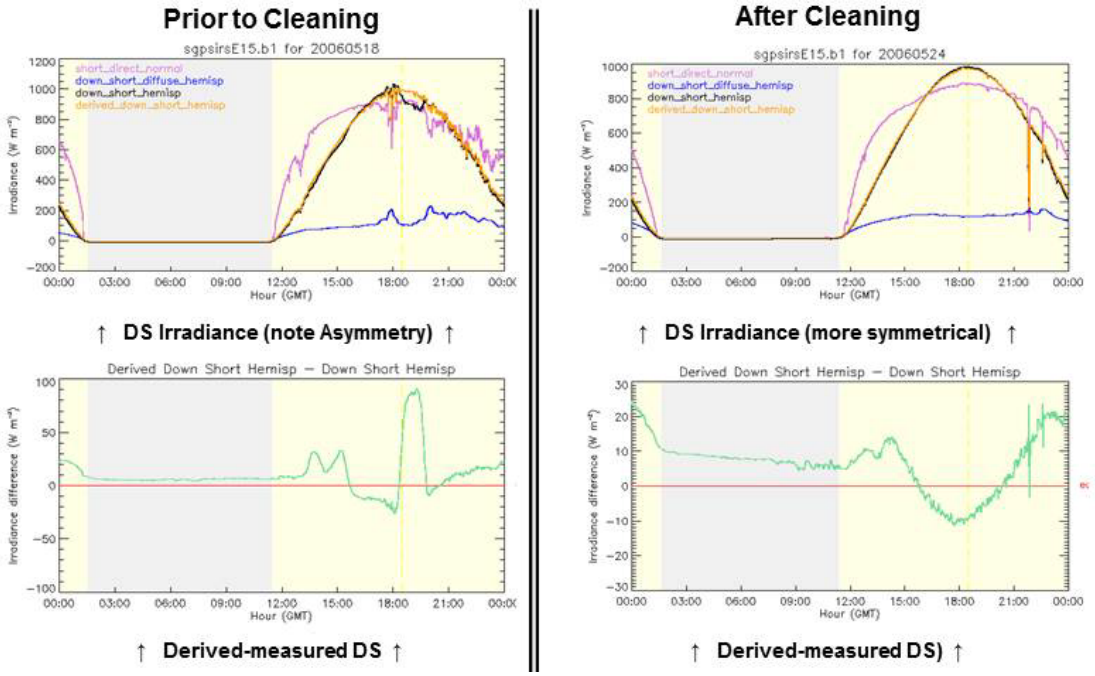

Figure 13. Dirty PSP dome.

5.3 User Notes and Known Problems

5.3.1 Incorrect Metadata

When radiometers are changed for recalibration or other reasons, the site operators immediately upload a new program containing the serial numbers and calibrations into the Campbell Scientific, Inc., data loggers dedicated to the SIRS,SKYRAD or GNDRAD. If this is done properly, the values for the observed geophysical parameters immediately have the correct calibration coefficients applied. These values are ingested in the 60-second data and no further processing is necessary to produce the estimates in geophysical units with correct calibrations. The 20-second data consist of raw values and are not affected by the choice of calibration coefficients or serial numbers. However, the metadata for the 60-s data are not updated with the new calibration coefficients and serial numbers until a special file produced daily at time 23:59 GMT by the logger are read at that time by the site data system. Hence, it is possible that up to nearly 24 hours of partially incorrect metadata will be generated. This problem could be overcome by a procedure of turning off the data ingest and correcting it whenever the sensors are replaced. All data collected to date have this problem, because such a procedure has not been implemented. The amount of time and effort to take such actions does not seem to be justified for this fairly minor source of misinformation. Additionally, the information needed to account for this discrepancy can be found by the interested data user on the SIRS Operations Management Information System (OMIS) site (http://www.ops.sgp.arm.gov/) or TWP OMIS (http://www.twppo.lanl.gov/ops/sdl/review.a4d). NSA operations are not available online. In the future all operations are expected to be logged in the Operations Status System (OSS) (https://oss.arm.gov/oss.php).

5.3.2 On Time Formats and Values of Downward Shortwave Hemispheric Radiation (P011004.2)

All SIRS data are recorded in UTC. This means local sunset will occur after 24:00 UTC in the summer as can be found, for example, in the data file sgpsirsC1.a1.20000601.000000.cdf. The large positive values are valid for the afternoon period. The negative values after sunset (and throughout the night, depending on the cloud cover) are typical of single black thermopile detectors used in the SIRS network (see Dutton, EG, JJ Michalsky, T Stoffel, BW Forgan, J Hickey, DW Nelson, TL Alberta, and I Reda. 2001. "Measurement of Broadband Diffuse Solar Irradiance Using Current Commercial Instrumentation with a Correction for Thermal Offset Errors." *Journal of Atmospheric and Oceanic Technology* 18(3): 297-306, doi:10.1175/1520-0426(2001)018<0297:MOBDSI>2.0.CO;2.) Prior to the use of Eppley Laboratory, Inc. Model 8-48 in February 2001, the diffuse shortwave and, to a lesser extent, the global irradiance, can be corrected for thermal offsets. In any event, I would treat the small (<15 Watts per sq meter) nighttime shortwave irradiances as '0.0' when computing the daily total irradiation values. We have programmed the Campbell Scientific, Inc. Model CR10X data loggers to output the measurements using the convention where midnight is recorded as 00:00:00 and the date reflects the start of a new 24-hour day. In Campbell-ese, the 4-digit code for 'Time Options' is 1110 for the SIRS program. SIRS 1-minute data for a particular date are then recorded from 00:00 to 23:59. For example, the data recorded for 10:05 are the averages, minima, maxima, and standard deviations of the 2-second samples beginning 10:04:02 and ending 10:05:00. During the first six months of 2012 the CR10X data loggers and their associated multiplexer were replaced with the CR3000 data logger as part of upgrade procedures.

5.3.3 Pyranometer Thermal Offsets

Broadband downwelling shortwave diffuse (sky) irradiance measurements available from SIRS prior to February 22, 2001 require adjustment for thermal offsets. After this date, all SIRS were providing diffuse irradiance data as measured with an Eppley Laboratory, Inc., Model 8-48 (black and white) pyranometer. The operational date of each SIRS in 1997/98 and the date and time of Model 8-48 installation in February 2001 can be found in Table 7.

As described above in the Description of Observational Specifications, these thermal or "zero" offsets refer to the generally reduced output signals from a shaded pyranometer due to the exchange of longwave (infrared) irradiance between the single black thermopile detector, the protective glass domes surrounding the detector, and the atmosphere. Originally considered an acceptable nighttime response of thermopile-type pyranometers, the generally negative bias is now recognized to significantly affect the accuracy of SIRS diffuse irradiance data during daylight periods.

Studies of the Eppley Laboratory, Inc. Model PSP (Precision Spectral Pyranometer), used for the SIRS measurements of diffuse irradiance, suggest the thermal offset correction can range from near 0 to as much as 30 Watts per square meter, depending on the coincident net longwave, or infrared irradiance [1, 2]. Under very clear-sky conditions, the diffuse irradiance from a shaded PSP can be less than the minimum physical limit defined by radiative transfer model estimates based only on Rayleigh scattering effects.

A correction method has been developed for adjusting SIRS diffuse irradiance data [3]. The resulting value-added product (VAP) will be applied to SIRS data for the period of this DQR. The VAP will not be applied to SIROS data collected before the instrument platform was converted to SIRS.

Additionally, the Model PSP radiometer has been replaced by a Model 8-48, which uses a black-and-white thermopile detector known to reduce the thermal offset errors to less than 2 Watts per square meter [3]. The radiometer replacement at this SIRS location was completed on the dates shown in Table 8.

Table 8. SIRS upgrade: Model 8-48 pyranometer installation for diffuse irradiance.

Site	SIROS to SIRS[2]	Model 8-48 Installation	Data Logger "OFF" (GMT)[3]	Returned to Service (GMT)[4]
C1	01-15-97	02-22-01	20:50	21:00
E1	11-20-97	02-13-01	20:15	20:25
E2	11-06-97	02-15-01	15:47	16:02
E3	11-04-97	02-14-01	19:30	19:50
E4	11-07-97	02-14-01	15:10	16:06
E5	11-06-97	02-14-01	19:45	20:03
E6	11-05-97	02-15-01	15:30	15:50
E7	10-31-97	02-13-01	19:25	19:45
E8	08-19-97	02-13-01	18:15	18:41
E9	02-06-98	02-13-01	15:40	16:00
E10	10-30-97	02-14-01	15:00	15:10
E11	08-20-97	02-20-01	20:40	21:05
E12	10-29-97	02-20-01	16:55	17:15
E13	08-25-97	02-22-01	20:21	20:35
E15	08-23-97	02-20-01	17:30	17:40
E16	08-21-97	02-21-01	16:20	16:50
E18	09-30-97	02-20-01	22:20	22:40
E19	06-16-98	02-22-01	15:35	15:48
E20	02-11-98	02-20-01	18:50	19:10
E21	07/22/99	02-20-01	21:00	21:35
E22	11-24-97	02-21-01	20:00	20:20
E24	11-25-97	02-22-01	16:15	16:35
E25	10-01-97	02-21-01	16:00	16:15

1 Information provided by Dan Nelson 2 Mar 99 and revised by Bev Kay 11 Apr 01 using OMIS.
2 Date SIRS was fully operational (assume 00:00 GMT).
3 Ending time for Data Quality Report (DQR) describing shaded PSP thermal offset remains uncorrected.
4 Time of data collection beginning with a new shaded Model 8-48 for Downwelling Diffuse (DD).

References:

[1] Gulbrandsen, A. 1978. "On the Use of Pyranometers in the Study of Spectral Solar Radiation and Atmospheric Aerosols." *Journal of Applied Meteorol*ogy 17(6): 899-904, doi:10.1175/1520-0450(1978)017<0899:OTUOPI>2.0.CO;2.

[2] Cess, RD, T Qian, and M Sun. 1999. "Consistency Tests Applied to the Measurement of Total, Direct, and Diffuse Shortwave Radiation at the Surface." *Journal of Geophysical Research – Atmospheres* 105(D20): 24881-24887, doi:10.1029/2000JD900402.

[3] Dutton, EG, JJ Michalsky, T Stoffel, BW Forgan, J Hickey, DW Nelson, TL Alberta, and I Reda. 2001. "Measurement of Broadband Diffuse Solar Irradiance Using Current Commercial Instrumentation with a Correction for Thermal Offset Errors." *Journal of Atmospheric and Oceanic Technology* 18(3) 297-314, doi:10.1175/1520-0426(2001)018<0297:MOBDSI>2.0.CO;2.

5.3.4 Exceeding Acceptable Measured versus Derived Limits

Derived values are calculated using the following three component formula:

$$DS = DNI * Cos(Z) + DD$$

where,

DS = Downwelling Hemispheric Shortwave (Global) Irradiance
DNI = Direct Normal Shortwave (Beam) Irradiance
Z = Solar Zenith Angle (sunrise/sunset = 90°)

There could be a difference in measured and derived values for irradiance outside of the empirical limit (- 10 W/m^2) at night, and during the day the values could differ from the calculated downwelling shortwave by about 20-30 W/m^2 (at times close to 50 W/m^2 difference). The difference would likely be due to the artifact of the cosine response of the particular installed PSP coupled with typical uncertainties of the current set of installed radiometers.

Also the unique variation of pyranometer responsivity (calibration factor) as a function of solar zenith angle and azimuth may play a factor in the discrepancy.

5.4 Frequently Asked Questions

Mentors and associates are directed to the ARM Data Quality Office Wiki provided they have a current ARM password (http://arm.physicstools.com/dqcms/bin/view/DQdocs/WebHome) for overview of the collection systems and common problems encountered with the instruments themselves (e.g., SIRS/GNDRAD/SKYRAD wikis). End users are directed to the appropriate end data product VAPs that will apply quality controls to ensure only high-quality data will be available to the data user.

6.0 Data Quality

6.1 Data Quality Health and Status

The following links go to current data quality health and status results

- DQ HandS (Data Quality Health and Status main page)
- Data Quality Explorer (Direct access to Data Plots and NCVweb)

The tables and graphs shown contain the techniques used by ARM's data quality analysts, instrument mentors, and site scientists to monitor and diagnose data quality.

6.2 Data Reviews by Instrument Mentor

SIRS Instrument mentors review the Data Quality Office's (DQO) weekly Data Quality Assessment Reports (DQAR). If a problem is detected, a Data Quality Problem Report (DQPR) is issued. The DQPR system is a web-based system by which the mentor, local site operations staff, and the DQO are informed

and communicate to resolve a data quality problem (e.g., instrument failure, data collection issue, etc.). A DQPR is typically initiated by the DQO or instrument mentor during data review. Data Quality Reports (DQR) are prepared by instrument mentors as needed to close out corresponding DQPRs.

6.3 Data Assessments by Site Scientist/Data Quality Office

All DQO and most Site Scientist techniques for checking have been incorporated within DQ HandS and can be viewed there.

7.0 Value-Added Procedures and Quality Measurement Experiments

Many of the scientific needs of the ARM Facility are met through the analysis and processing of existing data products into "value-added" products or VAPs. Despite extensive instrumentation deployed at the ARM CART sites, there will always be quantities of interest that are either impractical or impossible to measure directly or routinely. Physical models using ARM instrument data as inputs are implemented as VAPs and can help fill some of the unmet measurement needs of the ARM Facility. Conversely, ARM produces some VAPs not in order to fill unmet measurement needs, but to improve the quality of existing measurements. In addition, when more than one measurement is available, ARM also produces "best estimate" VAPs. A special class of VAP called a Quality Measurement Experiment (QME) does not output geophysical parameters of scientific interest. Rather, a QME adds value to the input datastreams by providing for continuous assessment of the quality of the input data based on internal consistency checks, comparisons between independent similar measurements, comparisons between measurements and modeled results, and so forth. For more information, see the VAPs and QMEs web page.

One VAP directly related to the SIRS datastream as well as GNDRAD and SKYRAD is the QCRAD VAP. This VAP was created to “assess the data quality, and to enhance data continuity, for the ARM radiation data collected at all ARM Central and Extended facilities.” It is suggested that ARM data users primarily obtain their data from the QCRAD VAP for best estimates of short- and longwave radiation as measured by SIRS, SKYRAD, and GNDRAD. Similar to the SERI QC QC flags in the b1 datastream, QCRAD also includes QC flags indicating if data is passing or failing and why. For the most recent detail of the ARM VAP data processing chain, see the ARM engineering webpage (https://engineering.arm.gov/pcm/Main.html), select the processes tab and filter list by name “qcrad”, select QCRAD under New Process list, and click on the hierarchy symbol for full details (Figure 14 below).

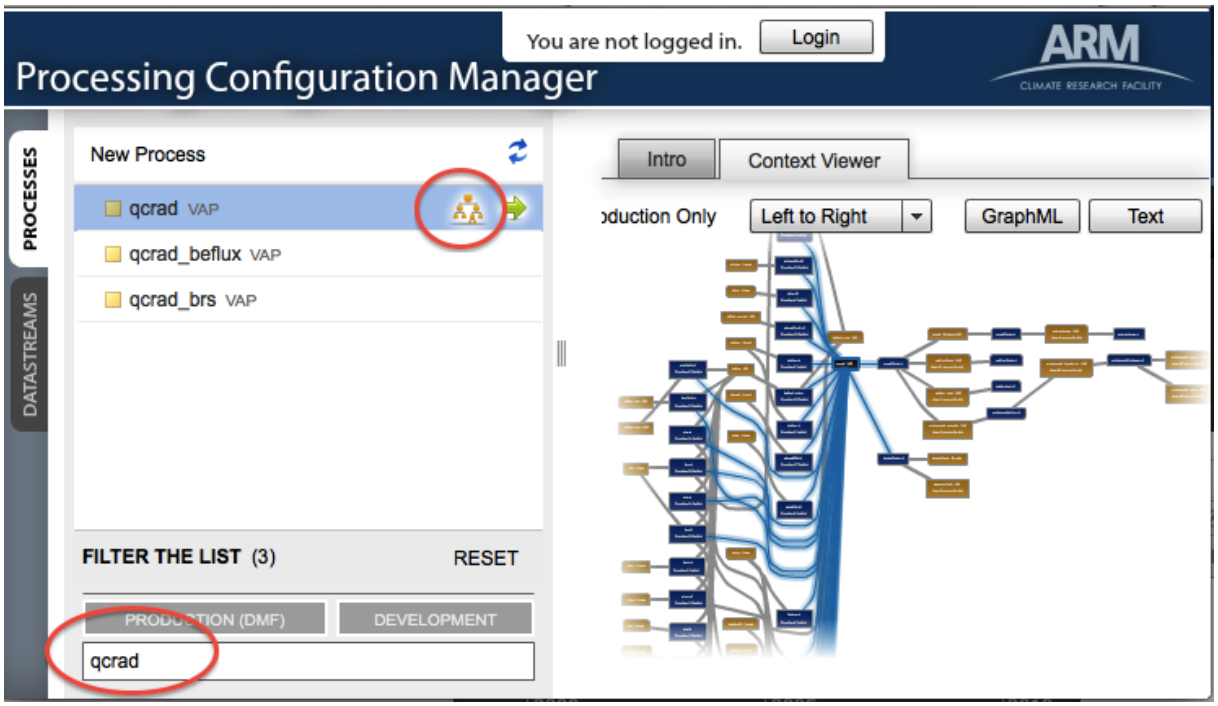

Figure 14. ARM data processing chain (QCRAD shown).

8.0 Instrument Details

8.1 Detailed Description

8.1.1 List of Components

The following radiometers manufactured by The Eppley Laboratory, Inc. in Table 9 are used at each SIRS/SKYRAD/GNDRAD station.

Table 9. Radiometers manufactured by The Eppley Laboratory, Inc.

Measurement	Radiometer Model	Mounting Arrangement	Typical Responsivity ($\mu V/Wm^{-2}$)	Typical Calibration Uncertainty[1]
Direct Normal	NIP	Solar Tracker	8.0	±2.5% or 2 Wm^{-2}
Diffuse Horizontal	8-48	[3] Shaded & Ventilated	9.0	±3.0% or 10 Wm^{-2}
Downwelling Shortwave	PSP	[3] Unshaded & Ventilated	9.0	±3.0% or 10 Wm^{-2}
Downwelling Longwave	PIR	Shaded & Ventilated	4.0	±2% or 2 Wm^{-2}
Upwelling Shortwave	PSP	[2] Inverted w/o ventilation	9.0	±3.0% or 10 Wm^{-2}

Measurement	Radiometer Model	Mounting Arrangement	Typical Responsivity ($\mu V/Wm^{-2}$)	Typical Calibration Uncertainty[1]
Upwelling Longwave	PIR	**Inverted w/o ventilation	4.0	±2% or 2 Wm^{-2}

[1] Field measurement uncertainties are larger and include the uncertainties associated with instrument calibration, installation, operation, and maintenance.

[2] At OLI and NSA the upwelling longwave and shortwave are ventilated and heated. SBS and TMP also had upwelling ventilator heaters.

[3] At OLI and NSA the downwelling ventilators are heated. SBS and TMP also had downwelling ventilator heaters.

8.1.2 System Configuration and Measurement Methods

Depending on the irradiance measurement, radiometers are mounted on either an automatic solar tracker or a stationary surface. The following abbreviations are used to describe the instrumentation:

DNI = Direct Normal (beam) Shortwave Irradiance
DD = Downwelling Diffuse (sky) Shortwave Irradiance
DS = Downwelling Total Hemispheric (global) Shortwave Irradiance
DIR = Downwelling Infrared (atmospheric) Irradiance
US = Upwelling Shortwave (reflected) Irradiance
UIR = Upwelling Infrared (terrestrial) Irradiance.

8.1.2.1 SIRS/BRS Configuration

The current SIRS/BRS data acquisition systems use Campbell Scientific, Inc. Model CR3000 data loggers, with each site using its own data logger. The SIRS and BRS CR3000 data loggers were installed during the first six months of 2012 as a system upgrade. Prior to the upgrade, the acquisition system consisted of a CR10X-1M with AM416 Multiplexer, 4 Mb memory card, and modem. The CR10X scanned all SIRS instruments once every two seconds with one-minute averages made available in the logger output tables for collection by the data system. The CR3000, now with enough channels to operate without a mux, can scan the instruments at the WMO recommended rate of once per second with one- minute averaged outputs. All components are inside a weather-resistant enclosure mounted above ground. The system is designed to operate over the full range of environmental conditions anticipated for the network of radiation stations (see http://www.campbellsci.com for detailed measurement and environmental specifications) and their relative locations shown in Figure 15:

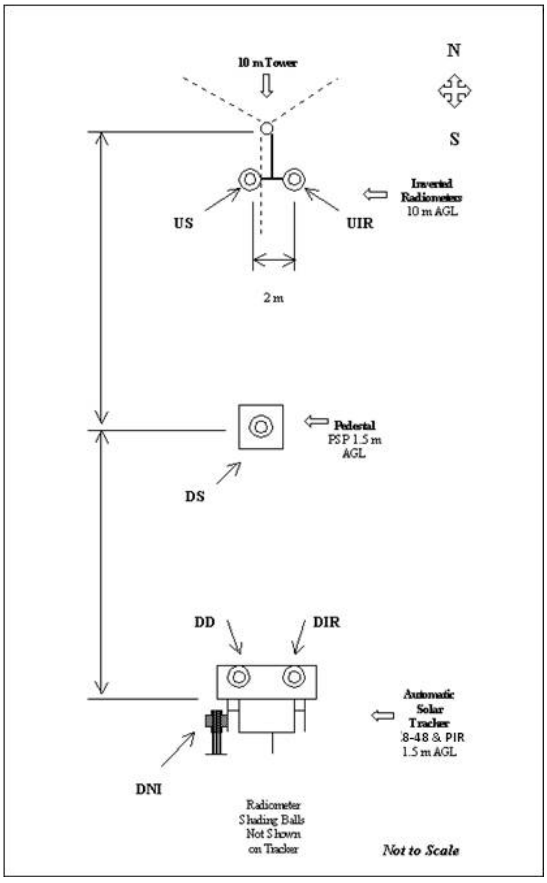

Figure 15. Example plan view of SIRS instrument locations.

The system is programmed to sample 10 inputs listed below every second and output the average, standard deviation, minimum, and maximum values of the six geophysical elements, described above, at the end of each minute. Appended to each 1-minute data output record are the instantaneous values sampled at 20 seconds, 40 seconds, and 60 seconds within the 1-minute interval. These values are compiled into Table 213 in logger memory and collected by the site data system commonly called the "EF computer". Additionally, at 23:59 each day, the instrument serial numbers and calibration factors used by the data logger program as well as station diagnostic information (logger program start time, running program name, data errors, etc.) are output in a separate Table 214 collected by the site data system once a day. The system can store up to two weeks of measured data and statistics, but the data are generally collected from the site data system by cellular modem every three hours.

8.1.2.2 SKYRAD/GNDRAD Configuration

The current SKYRAD/GNDRAD data acquisition systems use the Campbell Scientific, Inc. model CR3000 data logger. The SKYRAD/GNDRAD data loggers were originally Coastal Environmental Zeno data loggers installed from 1998 to 2004. To harmonize the solar measurement systems in the ARM network the Coastal loggers were replaced in 2004 with CR23X loggers. Additionally, as the AMFs were developed, they also shared the CR23X platform. However, starting in 2010 the SKYRAD/GNDRAD systems were upgraded to the CR3000. The SKYRAD/GNDRAD sites are separate sites, each operating with its own data logger.

8.1.2.3 Measurement Dictionary

1. DSTp = DS unshaded pyranometer thermopile output voltage (mV)
2. USTp = US inverted pyranometer thermopile output voltage (mV)
3. DDTp = DD shaded pyranometer thermopile output voltage (mV)
4. DNITp = DNI pyrheliometer thermopile output voltage (mV)
5. DIRTp = DIR pyrgeometer thermopile output voltage (mV)
6. DIRCr = DIR pyrgeometer case thermistor resistance (Kohm)
7. DIRDr = DIR pyrgeometer dome thermistor resistance (Kohm)
8. UIRTp = UIR pyrgeometer thermopile output voltage (mV)
9. UIRCr = UIR pyrgeometer case thermistor resistance (Kohm)
10. UIRDr = UIR pyrgeometer dome thermistor resistance (Kohm)

8.1.2.4 Reconstructing the 1-Minute Averages from Three 20-Second Samples

Use the average of the three samples for each of the elements described below to compute an average irradiance (W/sq m). The data acquisition system program uses these same procedures to compute the 1- minute statistics from the 2-second scans.

1. Global
   DS = DSTp (mV) * DS Cal Factor (W/sq m per mV)
2. Upwelling Shortwave
   US = USTp (mV) * US Calibration Factor (W/sq m per mV)
3. Diffuse
   DD = DDTp (mV) * DD Calibration Factor (W/sq m per mV)
4. Direct Normal
   DNI = DNITp (mV) * DNI Calibration Factor (W/sq m per mV)
5. Down/Upwelling Infrared (DIR or UIR)

   Step 1. Compute Temperature (K) from thermistor resistance (KOhm)

   $T = 1 / [A + BX + CX^3]$
   where,

   T = Temperature (K)
   A = 1.0295E-3
   B = 2.391E-4
   C = 1.568E-7
   X = ln(R*1000), and R = Resistance (KOhm)

Step 2. Compute Irradiance from PIR Temperatures (K) and Thermopile Voltages (mV)

$W_{in} = K_0 + K_1 * V_{TP} + K_2 * W_r + K_3 * (W_d - W_r)$

Where:

- K_0, K_1, K_2 and K_3 are calibration coefficients specific to each instrument
- V_{TP} is the thermopile output voltage in micro-Volt
- $W_d = \sigma * T_d^4$ =dome irradiance, in W/m^2,
  Where:
  - T_d = dome temperature, in Kelvin.
  - $\sigma = 5.6704 * 10^{-8}$, in $W/(m^2K^4)$
- $Wr = \sigma * T_r^4$ = receiver irradiance, in W/m^2,
  Where:
  - $T_r = T_c + K_4 * V_{TP}$ = receiver temperature, in Kelvin.
    Where $K_4 = 0.0007044$
  - T_c = Case temperature, in Kelvin.

8.1.3 Specifications

Selected theoretical measurement parameters of the SIRS radiometers are listed below in Table 10.

Table 10. Measurement limits of the SIRS radiometers.

Measurement	Radiometer Field of View	Wavelength Range (microns)	Typical Minimum Irradiance (Wm^{-2})	Typical Maximum Irradiance (Wm^{-2})
Direct Normal (beam) [DNI]	5.7°	0.3 to 3.0	0.0	1100
Diffuse Horizontal (sky) [DD]	2π sr	0.3 to 3.0	0.0	600
Downwelling Shortwave (global) [DS]	2π sr	0.3 to 3.0	0.0	1400
Downwelling Longwave (atmospheric) [DIR]	2π sr	3.5 to 50	50	800
Upwelling Shortwave (reflected) [US]	2π sr	0.3 to 3.0	0.0	1100
Upwelling Longwave (terrestrial) [UIR]	2π sr	3.5 to 50	100	800

8.1.4 Field of View and Angular Response

The SIRS pyrheliometer (Eppley Laboratory, Inc. Model NIP) field of view was designed to meet the World Meteorological Organization's design requirements circa 1960. Without the scattering effects of a clear atmosphere, the solar disc would appear to be about 0.5° at the earth's surface. The NIP geometry allows for solar tracker alignment tolerances possible at the time of the WMO specification and includes, therefore, an amount of circumsolar (forward scatter) radiation.

The SIRS pyranometers (Eppley Laboratory, Inc. Model PSP) have unique angular response characteristics that can be determined and verified with calibration (Stoffel, et al., 2010, pg. 12-13). The angular response of the pyranometer is a major contributor to the estimated measurement uncertainty for the various shortwave irradiance elements. Figure 16 illustrates calibration results with respect to zenith angle.

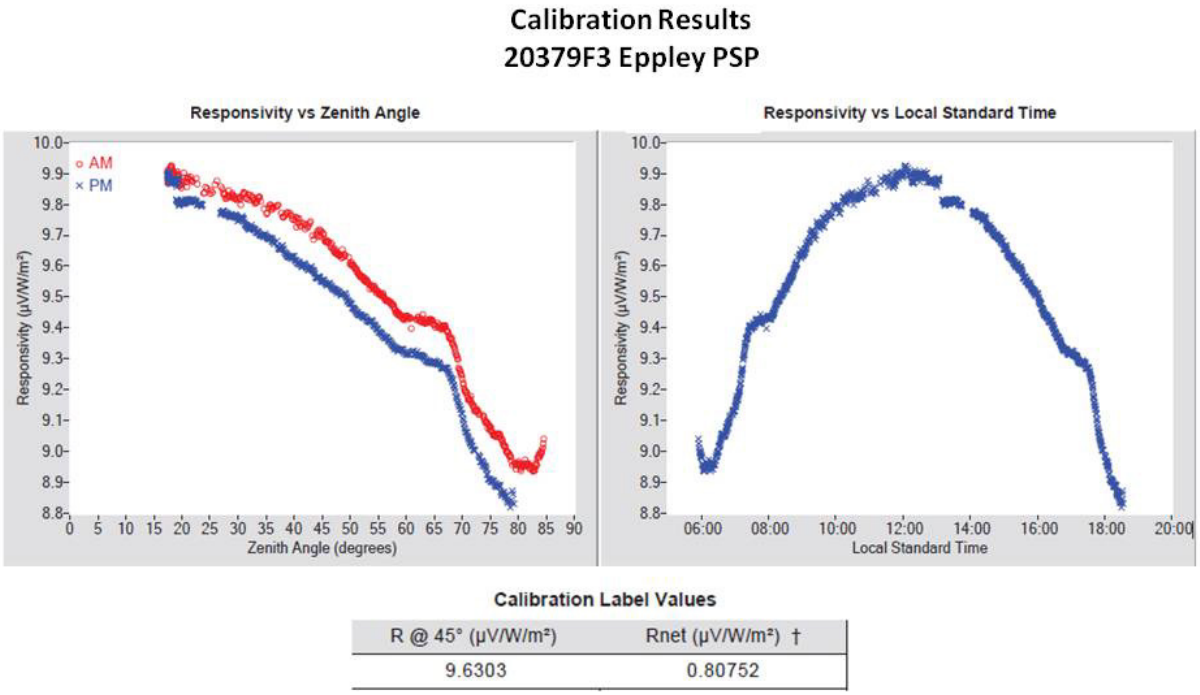

Figure 16. Pyranometer calibration results summarizing Rs versus SZA (left) and versus local standard time (right). Also shown is the calibration result at 45° (bottom).

8.1.5 Spectral Response

The spectral range in which the SIRS radiometers operate are listed in Table 10 above. The precise responsivities across that range vary with instrument model.

8.1.6 Thermal Offsets

Shortwave radiometers should produce a null signal in the absence of solar radiation. However, all commercially available pyranometers based on thermoelectric transducers exhibit a non-zero output signal in the absence of solar radiation. These signals are believed to be a result of thermal gradients within the pyranometer.

The Eppley Laboratory, Inc. Model PSP is a thermoelectric, single black detector design with well-established performance characteristics (Thekaekara 1972; Hulstrom 1989; McCluney 1994). As shown in Figure 17, the two Schott Glass hemispheres protect the thermopile detector from the weather. These inner and outer domes are also used to reduce the thermal exchange between the detector, or thermopile "hot" junction, and the environment. The body of the instrument is a relatively massive bronze casting that is used to control the "cold" or reference junction of the thermopile. Recent studies of this and other models of pyranometers suggest thermal offsets are producing as much as 30 Wm^{-2} during clear-sky, nighttime conditions. Similarly, daytime measurements of downwelling diffuse shortwave irradiance must be corrected for thermal offsets. ARM will use a correction method based on correlations with the net infrared and observed diffuse irradiances (Dutton et al., 2001).

Figure 17. Two Schott Glass hemispheres protect the thermopile detector from the weather.

8.1.6.1 AC to DC Fan Upgrade and Results

During 2014, a transition from AC fans to DC fans for PSP, 8-48, and PIR ventilators used in the SGP BORCAL and at SIRS and SKYRAD sites was performed under ECO-00991. The NSA and OLI site SKYRAD and GNDRAD ventilators have been using DC fans, and transition to the selected 12-volt DC fan model specified in ECO-00991 was planned to be done by site operators during the spring-summer 2015 period. This task has been completed at the SGP. Table 10 contains the fan transitions start dates and times for each site.

Table 11. AC to DC fan transition dates.

AC to DC Fan Transition Dates	
Site	Date
C1 (SGP - BRS)	7/25/2014
C1 (SGP - Test bed)	7/16/2014
E9 (SGP)	7/14/2014
E11 (SGP)	7/24/2014
E12 (SGP)	7/23/2014
E13 (SGP)	8/26/2014
E15 (SGP)	7/18/2014
E21 (SGP)	7/8/2014
E31 (SGP)	7/10/2014
E32 (SGP)	7/15/2014
E33 (SGP)	8/14/2014
E34 (SGP)	8/15/2014
E35 (SGP)	8/18/2014
E36 (SGP)	8/19/2014
E37 (SGP)	8/22/2014
E38 (SGP)	8/20/2014
TWP C1 (Darwin)	9/8/2014
ENA (Azores)	12/21/2014
MAO AMF1 (Brazil)	2/5/2015
NSA*	Planned for spring-summer, 2015
OLI*	Planned for spring-summer, 2015
*Currently running on DC fans, but they are not the designated model.	

Some examples of the results of the ventilator fan upgrade for two sites (C1 and E13) for both the PSP and the 8-48 are shown in Figure 18. A summary of the results of the ventilator fan upgrade at 18 sites are summarized in Table 11.

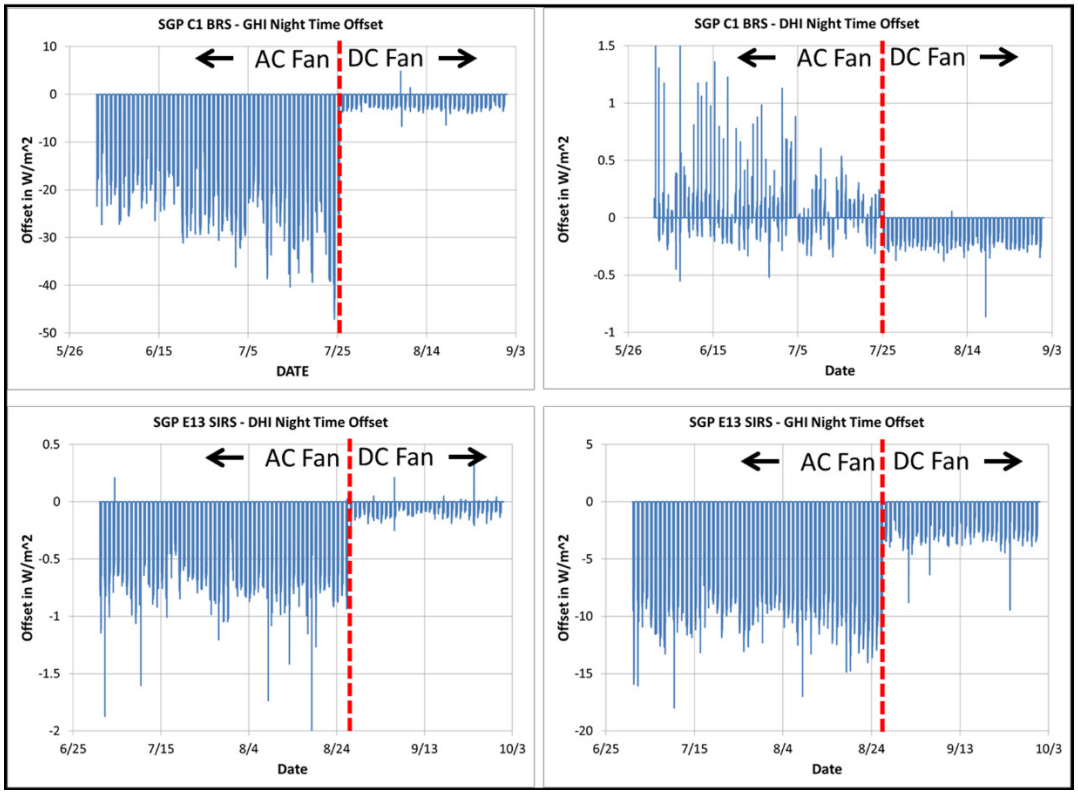

Figure 18. Nighttime offset reduction results from AC to DC fan transition for SGP C1 and SGP E13.

Table 12. Summary of resulting reduction in nighttime offset for the PSP and 8-48 at 18 sites.

PSP Offset Thermal Reduction Summary			
Minimum change W/m^2 (C1-Test)	Maximum change W/m^2 (C1-BRS)	Average before change W/m^2 (All sites)	Average after Change W/m^2 (All sites)
1.9	19.2	-7.2	-2.3
8-48 Offset Thermal Reduction Summary			
Minimum change W/m^2 (E37)	Maximum change W/m^2 (E31)	Average before change W/m^2 (All sites)	Average after Change W/m^2 (All sites)
1.3	3.2	-0.7	-0.3

8.2 Theory of Operation

8.2.1 Shortwave Irradiance

Three pyranometers are positioned to measure the hemispheric irradiance fields:

DS – Unshaded, ventilated, and mounted in horizontal orientation
US – Inverted, unventilated and mounted 10m above the ground level
DD – Shaded, ventilated, and mounted on automatic solar tracker in horizontal orientation.

A single pyrheliometer is mounted on an automatic solar tracker and aligned to the sun's disc.

The following relationships are expected from the SIRS measurement system for the various broadband shortwave irradiance elements.

$$DS = DNI * Cos(Z) + DD$$
$$US = DS * \rho$$
$$DS \leq ETR$$
$$DNI \leq ETRN$$

Where,

DS = Downwelling Hemispheric Shortwave (Global) Irradiance
DNI = Direct Normal Shortwave (Beam) Irradiance
Z = Solar Zenith Angle (sunrise/sunset = 90°)
DD = Downwelling Diffuse Shortwave (sky) Irradiance
US = Upwelling Diffuse Shortwave (reflected) Irradiance
ρ = Surface Shortwave Albedo (typically 0.2 for vegetation, 0.8 for fresh snow)
ETR = Extraterrestrial (exo-atmospheric) Radiation on horizontal surface
ETRN = Extraterrestrial Radiation Normal (beam) to the sun (1366 ±5 Wm^{-2}).

8.2.2 Longwave Irradiance

The accepted equation for computing incoming infrared radiation from a pyrgeometer is:

$$W_{in} = K_0 + K_1 * V_{TP} + K_2 * W_r + K_3 * (W_d - W_r)$$

Where:

- K_0, K_1, K_2 and K_3 are calibration coefficients specific to each instrument
- V_{TP} is the thermopile output voltage in micro-Volt
- $W_d = \sigma * T_d^4$ =dome irradiance, in W/m^2,

  Where:

  - T_d = dome temperature, in Kelvin.
  - $\sigma = 5.6704 * 10^{-8}$, in $W/(m^2K^4)$

- $Wr = \sigma * T_r^4$ = receiver irradiance, in W/m^2,
  Where:
  - $T_r = T_c + K_4 * V_{TP}$ = receiver temperature, in Kelvin.
    Where $K_4 = 0.0007044$
  - T_c = Case temperature, in Kelvin.

Historically, the SIRS pyrgeometer output was not calculated exactly from this equation since there is no calibration of the pyrgeometer done at the ARM facility and thus no measured K_0, K_1, K_2 K_3, and K_4. Instead, the Eppley responsiveness is used along with theoretical values for the five calibration coefficients discussed above. Namely,

$K_0 = 0$
$K_1 = 1/$ (Eppley Responsiveness)
$K_2 = 1$
$K_3 = -4$
$K_4 = 0$

Substituting these theoretical values for K_0, K_1, K_2, K_3, and K_4 and the above definitions for W_r and W_d into the original equation above yields the following equation, which is used to compute the IR for the pyrgeometers:

$$IR = K_1 * V_{tp} + \sigma * T_C^{\,4} + 4 * \sigma * (T_d^{\,4} - T_C^{\,4})$$

Recently, a new method for determining the K_0, K_1, K_2, and K_3 terms has been developed. This process is discussed in section 8.3.3.

8.3 Calibration

8.3.1 Theory

The calibration of all SIRS shortwave radiometers (pyrheliometers and pyranometers) is traceable to the World Radiometric Reference (WRR) maintained by the World Radiation Center (WRC) for the World Meteorological Organization. Calibrations are performed at the SGP Radiometer Calibration Facility (RCF–see separate entry) using the Broadband Outdoor Radiometer CALibration (BORCAL) methods developed at NREL. A group of three electrically self-calibrating absolute cavity radiometers is maintained by NREL as the reference standards for the U.S. Department of Energy (DOE) and ARM. WRR calibration traceability of these reference standards is maintained for all DOE programs by participation in the International Pyrheliometer Comparisons (IPC) held every five years at the WRC. NREL Pyrheliometer Comparisons (NPCs) are held annually at the Solar Radiation Research Laboratory (SRRL) in Golden, Colorado to transfer the WRR to participating instruments and ensure the measurement performance of the reference standards.

The calibration of all SIRS longwave radiometers is traceable to The Interim World Infrared Standard Group (WISG).

8.3.2 Shortwave Radiometer Calibrations

The *Component Summation Method* used for all BORCAL events is a modified version of the shading method described in the American Society for Testing and Materials (ASTM) Standard E913-82, "Standard Method for Calibration of Reference Pyranometers with Axis Vertical by the Shading Method."

The direct normal (beam) irradiance is measured with one or two absolute cavity radiometers, and the diffuse (sky) irradiance is measured with two pyranometers shaded with a tracking disk (Figure 19 and Figure 20). The two pyranometers providing the reference diffuse irradiance are calibrated at NREL/SRRL prior to SGP's BORCAL event.

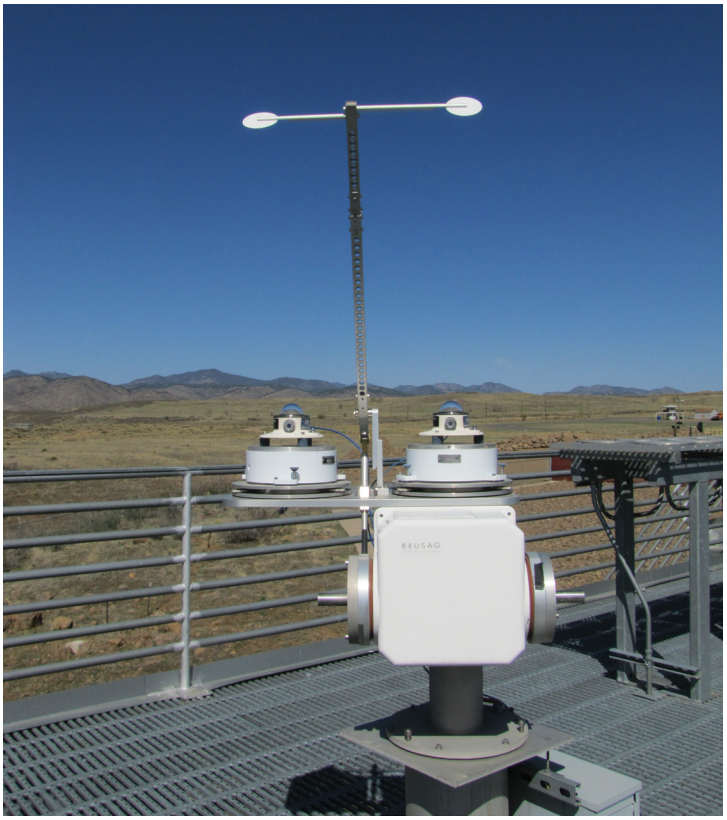

Figure 19. Two pyranometers shaded with a tracking disk.

The responsiveness for a pyrheliometer is calculated for each data point by dividing the value of the instrument's output signal (microvolts) by the mean value of the absolute cavity radiometer(s) output (W/sq m).

The responsiveness for a pyranometer is calculated by dividing the value of the instrument's output signal (microvolts) by the computed reference global horizontal irradiance (W/sq m). The computed reference irradiance is the sum of the diffuse radiation and the vertical component of the direct beam irradiance (cavity radiometer irradiance multiplied by the cosine of the solar zenith angle at the time of measurement). This assumes that the pyranometer has a perfect angular response. The solar zenith angle calculations are corrected for atmospheric refraction effects at the calibration facility.

During a calibration event, one or more pyranometers (The Eppley Laboratory, Inc. Model 8-48) and pyrheliometers (The Eppley Laboratory, Inc. Model NIP) are used as control standards to monitor the calibration process.

Figure 20. Component summation calibration.

8.3.3 Longwave Radiometer Calculations

A method for pyrgeometer calibrations was developed at the SGP RCF, under ECO-00781, which is based on outdoor measurements. Prior to this development, a blackbody was used for LW calibrations with a period of time where the manufacturer's calibration was used. The new method was implemented in 2015 and as of March, 2018 over 600 LW calibrations have been performed. The instruments under calibration are deployed outdoors and collocated with two reference pyrgeometers. During the calibration event the test instruments are deployed outdoors long enough to capture data during all sky conditions (cloudy, partly cloudy, and clear skies) during the nighttime hours (zenith >96°). A linear regression is used to calculate the calibration coefficients for all test instrument, i.e., K_0, K_1, K_2, and K_3 (see section 8.2.2). The calibration certificate is provided with two equations for determining the longwave irradiance, one which uses the K_0 term and one which does not. These two equations are:

$$W_{in} = K_0 + K_1 * V_{TP} + K_2 * W_r + K_3 * (W_d - W_r)$$

$$W_{in} = K_1 * V_{TP} + K_2 * W_r + K_3 * (W_d - W_r)$$

8.3.4 Procedures

Calibration procedures as well as quality control measures are controlled by the instrument mentor and are periodically reviewed to ensure proper adherence to accepted industry practices. Currently, calibration procedures at SGP are nearly identical to those performed at NREL's SRRL.

8.3.5 History

Pyranometers and pyrheliometers are recalibrated annually at the SGP Radiometer Calibration Facility (RCF). Calibration results and instrument deployment records are available from NREL's ARM Instrument Management (AIM) System at http://www.nrel.gov/aim/.

8.4 Operation and Maintenance

8.4.1 User Manuals/Instrument Information

PSP – Precision Spectral Pyranometer
(http://s.campbellsci.com/documents/us/manuals/psp.pdf)

8-48 – Black & White Pyranometer
http://eppleylab.com/instrumentation/black_white_pyranometer.htm

NIP
http://eppleylab.com/instrumentation/normal_incidence_pyrheliometer.htm

PIR
http://eppleylab.com/instrumentation/precision_infrared_radiometer.htm

2AP
http://www.kippzonen.com/Product/21/2AP-Sun-Tracker#.Upzyy8RDuSo

CR3000
http://www.campbellsci.com/cr3000

8.4.2 Software Documentation

ARM netCDF file header descriptions may be found at SIRS Data Object Design Changes.

8.4.3 Additional Documentation

To provide research-quality irradiance measurements, the SIRS radiometers are recalibrated annually. The existing radiometer inventory allows for 50% spares, reducing the down time for station operation due to calibration. Maintenance of the SIRS equipment (i.e., cleaning, preventive maintenance, corrective maintenance) is performed during the biweekly visits to the SGP facilities. Detailed information is available from the SGP Operations Management Information System (OMIS) website. Additionally, SKYRAD, GNDRAD operations events are logged in the ARM OSS system.

8.5 Glossary

See the ARM Glossary.

8.6 Acronyms

See the ARM Acronyms and Abbreviations.

8.7 Citable References

BIPM. 1995. Guide to the Expression of Uncertainty in Measurement. Published by ISO TAG 4, 1993 (corrected and reprinted, 1995) in the name of the BIPM. ISBN 92-67-10188-9, 1995. 1995 BIPM, IEC, IFCC, ISO, IUPAC, IUPAP and OIML.

Cess, RD, T Qian, and M Sun. 2000. "Consistency tests applied to the measurement of total, direct, and diffuse shortwave radiation at the surface." *Journal of Geophysical Res*earch – *Atmospheres* 105(D20): 24881-24887, doi:10.1029/2000JD00402.

Coulson, KL. 1975. *Solar and Terrestrial Radiation Methods and Measurements*. Academic Press, New York, New York. ISBN 0-12-192950-7.

Dutton, EG, JJ Michalsky, T Stoffel, BW Forgan, J Hickey, DW Nelson, TL Alberta, and I Reda. 2001. "Measurement of Broadband Diffuse Solar Irradiance Using Current Commercial Instrumentation with a Correction for Thermal Offset Errors." *Journal of Atmospheric and Oceanic Technology* 18(3): 297-314, doi:10.1175/1520-0426(2001)018<0297:MOBDSI>2.0.CO;2.

Gulbrandsen, A. 1978. "On the Use of Pyranometers in the Study of Spectral Solar Radiation and Atmospheric Aerosols." *Journal of Applied Meteorol*ogy 17(6): 899-904, doi:10.1175/1520-0450(1978)017<0899:OTUOPI>2.0.CO;2.

Hickey, JR, and AR Karoli. 1974. "Radiometer Calibrations for the Earth Radiation Budget Experiment." *Applied Optics*13(3) 523-533, doi:10.1364/AO.13.000523.

Hickey, JR. 1975. "Solar Radiation Measuring Instruments: Terrestrial and Extraterrestrial." *Proceedings of the Society of Photo-Optical Instrumentation Engineers* 68, *Optics in Solar Energy Utilization*, Y.H. Katz (ed.). ISBN 0892520809.

Hill, AN, JR Latimer, AJ Drummond, and HW Greer. 1966. "Standardized Procedures in the North American Continent for the Calibration of Solar Radiation Pyranometers." *Solar Energy* 10(4): 184.

Hulstrom, RL. 1989. *Solar Resources*. The MIT Press, Cambridge, Massachusetts. ISBN 0-262-08184-9.

Iqbal, M. 1983. *An Introduction to Solar Radiation*. Academic Press, New York, New York. ISBN 0-12-373750-8 (ISBN 0-12-373752-4 for paperback).

Karoli, AR, JR Hickey, and RG Frieden. 1983. "Self-calibrating Cavity Radiometers at the Eppley Laboratory: Capabilities and Applications." *Proceedings of SPIE-The International Society for Optics and Photonics* 416: 43-49, doi:10.1117/12.935917.

Kutchenreiter, M, M Dooraghi, I Reda, A Habte, A Andreas, M Sengupta, and M Anderberg. 2015. "Ventilator DC fan upgrades and evaluation at NREL." Vienna, Virginia, March 16-19.

Kutchenreiter, M, P Gotseff, A Habte, I Reda, M Sengupta, A Andreas, and M Anderberg. 2014. "Evaluation of DC ventilator fans proposed for pyranometer measurements in the ARM Facility." Atmospheric System Research (ASR) Science Team Meeting, Potomac, Maryland.

Latimer, JR. 1964. "An Integrating Sphere for Pyranometer Calibration." *Journal of Applied Meteorology* 3(3), 323-326, doi:10.1175/1520-0450(1964)003<0323:AISFPC>2.0.CO;2.

Maxwell, EL, and DR Myers. 1992. "Daily estimates of aerosol optical depth for solar radiation models." *Solar '92, Proceedings of the Annual Meeting, American Solar Energy Society*, p. 323. Cocoa Beach, Florida, June 15-18.

McCluney, WR. 1994. *Introduction to Radiometry and Photometry*. Artech House, Inc., Norweed, Massachusetts. ISBN 0-89006-678-7.

Michalsky, J, M Kutchenreiter, and C Long. 2017. "Significant improvements in pyranometer nighttime offsets using high-flow DC ventilation." *Journal of Atmospheric and Oceanic Technology* (34(6): 1323-1332, doi:10.1175/JTECH-D-16-0224.1.

Myers, DR, KA Emery, and TL Stoffel. 1989. "Uncertainty estimates of global solar irradiance measurements used to evaluate PV device performance." *Solar Cells* 27(1-4): 455-464, doi:10.1016/0379-6787(89)90055-0.

Reda, I. 2011. Method to Calculate Uncertainty Estimate of Measuring Shortwave Solar Irradiance using Thermopile and Semiconductor Solar Radiometers. NREL Report No. TP-3B10-52194

Reda, I, J Zeng, J Scheuch, L Hanssen, B Wilthan, D Myers, and T Stoffel. 2012. "An absolute cavity pyrgeometer to measure the absolute outdoor longwave irradiance with traceability to international system of units, SI." *Journal of Atmospheric and Solar-Terrestrial Physics* 77: 132-143, doi:10.1016/j.jastp.2011.12.011.

Reda, I. 1999. Improving the Shade/Unshade Method to Calculate the Responsivities of Solar Pyranometers. NREL Report No. TR-26483.

Taylor, BN, and CE Kuyatt. 1993. Guidelines for Evaluation and Expressing the Uncertainty of NIST Measurement Results. NIST Technical Note 1297. National Institute of Standards and Technology.

Thekaekara, MP, RH Collingbourne, and AJ Drummond. 1972. "A Comparison of Working Standard Pyranometers." *Bulletin of the American Meteorological Society* 53(1): 8-15.

World Meteorological Organization. 1971. *Guide to Meteorological Instrument and Observing Practices*. 4th edition, WMO-No. 8, TP. 3, Geneva, Switzerland. (Note: Most WMO publications are available in the U.S. from the American Meteorological Society, Boston, Massachusetts.

Appendix A

SERIQC Methodology

Up until early 2012, each 1-minute irradiance value in the SIRS b1 datastream was assigned a two-digit data quality flag based on the results of automated assessments developed by the National Renewable Energy Laboratory (NREL). This system was called SERI QC. When the SIRS ingest was ported to Linux in early 2012 the SERI QC system was dropped in favor of a simplified max/min/delta QC flag system. Users are now directed to the QCRAD Value-Added Product (VAP) available for all SIRS/SKYRAD and GNDRAD sites. Section 7 contains additional background and links for this product. The SERI QC information that follows in this section is still relevant to archived SIRS datastreams prior to 2012.

Each 1-minute irradiance value is assigned a two-digit data quality flag (00-99) based on the results of automated assessments developed by NREL. Shortwave irradiance tests are based on the *SERI-QC* process developed by the Solar Energy Research Institute – SERI (now NREL). A description of this automated quality assessment tool can be found at the NREL Renewable Resource Data Center.

The ARM Facility has incorporated the SERI QC concepts and upgraded the automated capabilities to include the upwelling shortwave and all longwave irradiances, thereby addressing each of the SIRS data elements. Information about the resulting *Data Quality Management System Version 3*.0 *(DQMS-3)* can be found in the ARM Publications.

Additional elements of *DQMS-3* are used for assessing SIRS data quality and providing the means for correcting known instrumentation responses:

1. *DQMS-3* converts 1-minute broadband shortwave irradiance data from flux densities in Watts per square meter to non-dimensional units normalized to the coincident extraterrestrial (exoatmospheric) values:

    a. K_T = Total Hemispheric / Extraterrestrial = DS / ETR

    b. K_N = Direct Normal / Extraterrestrial Normal = DNI / ETRN

    c. K_D = Downwelling Diffuse / Extraterrestrial = DD / ETR

    d. Resulting in the relationship among the three measured shortwave components:

i. $K_T = K_N + K_D$
[eq. 4]

e. Failing the above "3-component" test, pairs of irradiance data can be evaluated using the transformation.

f. When presented in K-Space, the data can be evaluated based on acceptable limits determined by physical limits, internal consistency, and careful inspection of historical data. Typical bounds are shown in Figure 21.

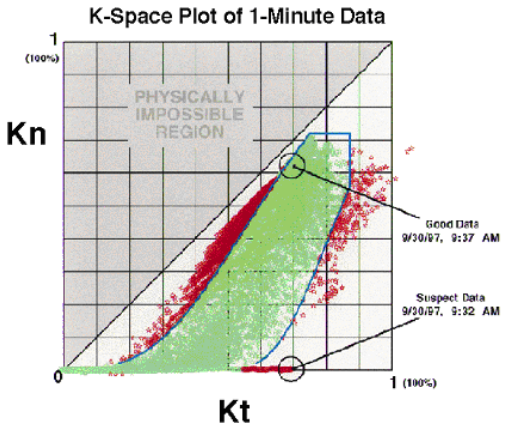

Figure 21. Typical acceptable bounds of Normalized Total Hemispheric and Direct Normal irradiance.

DQMS-3 assigns a two-digit quality flag to each irradiance data element based on the location in the appropriate K-Space coordinates.

Table 13. DQMS-3 flagging convention (based on SERI_QC methodology).

Flag	Description
00	Untested (raw data)
01	Passed one-component test; data fall within max-min limits of Kt, Kn, or Kd
02	Passed two-component test; data fall within 0.03 of the Gompertz boundaries
03	Passed three-component test; data come within ±0.03 of satisfying Kt=Kn+Kd
04	Passed visual inspection; *not used* by SERI_QC
05	Failed visual inspection; *not used* by SERI_QC
06	Value estimated; passes all pertinent SERI_QC tests
07	Failed one-component test; lower than allowed minimum
08	Failed one-component test; higher than allowed maximum
09	Passed three-component test but failed two-component test by > 0.05 (K-units)
10-93	Failed two- or three-component tests in one of four ways. To determine the test failed and the manner of failure (high or low), examine the remainder of the calculation (flag + 2) / 4. Rem Failure:

Flag	Description
	0 Parameter too low by three-component test (Kt = Kn + Kd) 1 Parameter too high by three-component test (Kt = Kn + Kd) 2 Parameter too low by two-component test (Gompertz boundary) 3 Parameter too high by two component test (Gompertz boundary) The magnitude of the test failure (distance in K-units) is determined from: D = INT ((flag + 2) / 4) / 100.
94-97	Data fall into a physically impossible region where Kn > Kt by K-space distances of 0.05 to 0.10 (94), 0.10 to 0.15 (95), 0.15 to 0.20 (96), and ≥0.20 (97)
98	Not used
99	Missing data

More detailed information about SERI QC is available from the **NREL Renewable Resource Data Center**.

Appendix B

PSP, 8-48, and PIR Ventilator Flow Maintenance

This addendum to the SIRS Handbook applies to Eppley Model VEN ventilators used with Eppley radiometers operated by the ARM Climate Research Facility. Information and photographs pertaining to activities to perform for the reduction of airflow leakage and restriction are provided.

Locations: ARM facilities performing SIRS, SKYRAD, GNDRAD, and BRS measurements.

Affected Instruments: Downwelling PSP, 8-48, PIR; Upwelling PSP and PIR operated at NSA, OLI, and AMF cold-climate deployments.

Description: At the affected locations indicated above, the downwelling PSP, 8-48, and PIR radiometers, plus upwelling PSP and PIR radiometers at cold-climate locations, are operated with Eppley Model VEN ventilators. Operation of the radiometers with ventilators is intended to improve the reliability and accuracy of measurements by the reduction of accumulation of dust, dew, and frost that would otherwise disturb the measurement. Additionally, the use of ventilators is intended to reduce thermal offset response.

It has been observed during field operations that the desired amount of airflow through the ventilators can sometimes become reduced. Reduced flow may typically be associated with leakage or airflow intake restriction. Leakage can typically occur at the location of the cable slot and also if an air gap exists between the bottom of the sun shield and the top edge of the upper clear plastic ventilator housing. Restriction of ventilation airflow may occur when the fan filter has excessive accumulations of dust or other material on the intake surface, or if there is inadequate spacing between the bottom edge of the white ventilator housing base and the top surface of the mounting plate.

Airflow Leak Reduction: Figure 22 indicates the location of the cable slot, a common point for leakage of fan output flow, resulting in reduced flow over the dome. This slot may be plugged using a piece of adhesive vinyl foam ("weather strip") tape or similar material. Figure 23 shows a piece of ¾-inch-wide, 3/16-inch-thick vinyl foam tape that has been cut, folded with the adhesive side together, and trimmed to fit within the cable slot. Note that PIR ventilators have a slightly wider cable slot opening, requiring an additional folded layer. Close attention is necessary to confirm proper sealing between the cable jacket and the sides of the cable slot, especially if the slot has been modified to be wider, or has uneven dimensions.

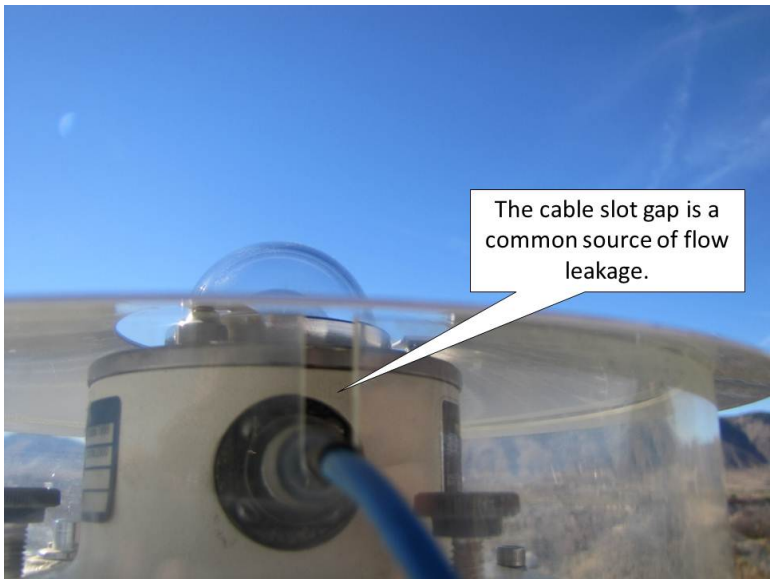

Figure 22. Open cable slot is source of slow leakage.

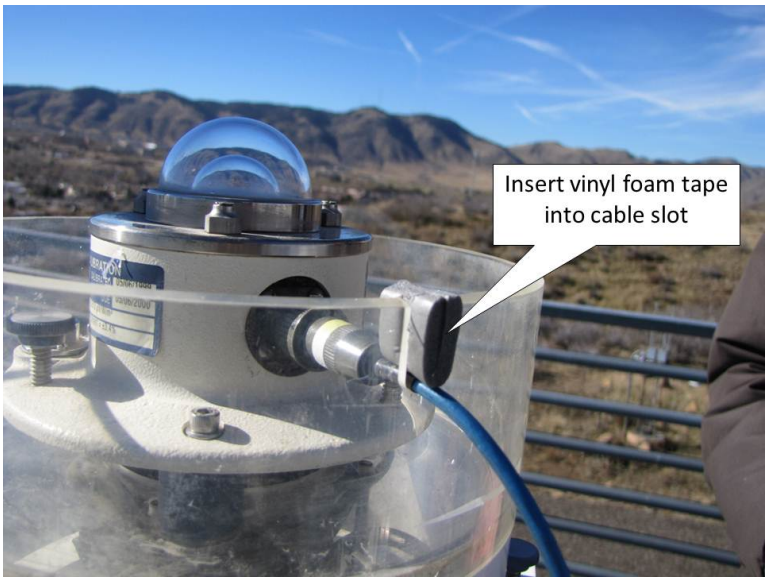

Figure 23. Plugging the slot with foam.

Figure 24 shows the location where the bottom of the sun shield and the top edge of the clear plastic meet. Perform a careful visual inspection around the entire circumference to identify any areas where a visible gap may exist. If a gap is present due to a slight deformation of the sun shield or some other cause, ventilation airflow can leak out through the gap, reducing flow over the dome. If the gap cannot be corrected by slight re-bending of the sun shield to its proper shape, a new replacement sun shield should be installed. An alternative to replacement of the sun shield entails the use of vinyl foam tape applied to the outer clear plastic surface along the circumference where the top plastic rim and bottom of the sunshield meet, to form a sealing band. Use sufficient upward positioning that will provide an air seal, but

not force the sun shield upward. Replacement of bent sun shields with shields free of deformations that could allow leakage is generally the recommended alternative.

Figure 24. Inspecting for gaps under the sun shield.

Reduction of Airflow Restrictions: The two common causes of airflow restriction are 1) excess accumulation of dust and other airborne material on the fan filter intake surface, and 2) inadequate spacing between the bottom edge of the ventilator housing base and the mounting plate. Figure 25 shows an easily visible accumulation of material on the intake surface of the fan filter. Removal of the accumulated deposits using a brush and portable vacuum is shown in Figure 26, resulting in a cleaned filter surface as shown in Figure 27. The necessary frequency for filter cleaning depends on local conditions and the amount of dust or other airborne matter in the ambient air. Visual checks of the filter should be made frequently enough to avoid buildup of accumulations on the filter intake surface that would result in an excessive airflow reduction. Quarterly cleaning is currently the acceptable best practice but frequency can increase depending on local site conditions (e.g., SGP/EF facilities located in active cultivated fields).

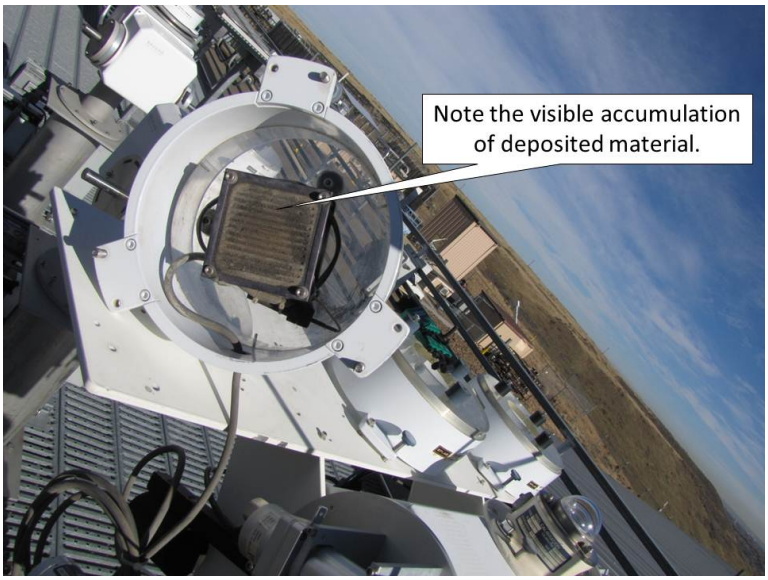

Figure 25. A dirty ventilator filter.

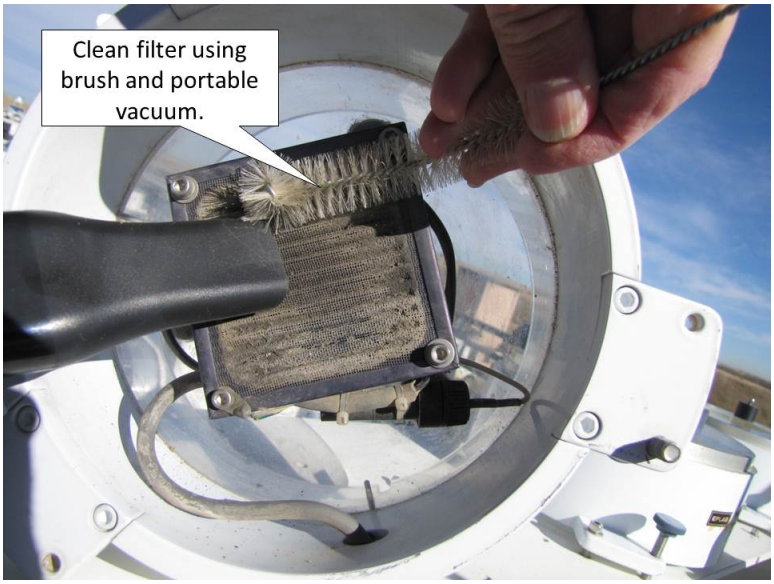

Figure 26. Cleaning the ventilator filter.

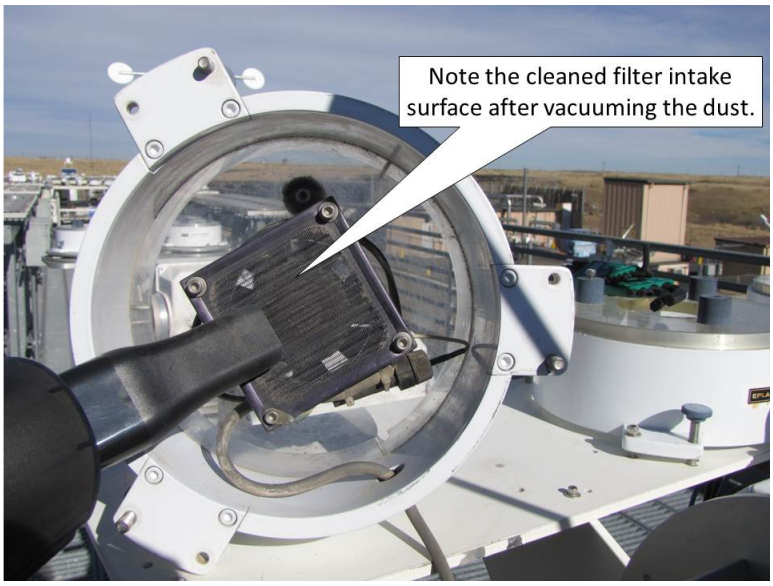

Figure 27. A cleaned ventilator filter.

To avoid improper restriction of intake airflow into the bottom inlet portion of the ventilator housing, a minimum spacing of 1 cm should exist between the bottom edge of the ventilator housing base and the mounting plate surface. Confirm that the radiometer circular level indicates correct leveling after any ventilator height adjustments. On tracker mounting plates, also confirm that the spacing is not set excessively high, in order to avoid incorrect shading.

The fan blades, fan frame surfaces, and ventilator interior surfaces are also areas where dust and other material can accumulate. When performing fan filter checks and maintenance, also inspect these areas and remove excess accumulated deposits. Also during site visits, remove accumulations of snow that may be present either on the top or around the sides and bottom area of the ventilator.

Flow Checks and Additional Maintenance: During each site inspection, the ventilator output airflow over the dome should be checked to confirm proper flow. The flow should be initially checked by the station operator in order to establish a 'reference flow', by holding a hand one inch above the dome to subjectively determine the force of the output flow when the fan filter is clean and any airflow leaks and restrictions have been corrected. Flow checks should be performed during each station inspection to determine if there is a reduction from the initial 'reference flow'. If there is a noticeable reduction in the ventilator output flow over the dome, investigate the cause and perform corrective maintenance. Also during station inspections, always perform a visual check of each radiometer and ventilator to ensure that radiometer domes, sun shields, and ventilator housings are correctly positioned and in proper operating condition to ensure proper ventilation flow and that improper airflow leakage is not occurring. The positioning of the radiometer and sun shield should provide an even circumferential spacing between the inner diameter of the opening of the sun shield and the radiometer dome. Any unevenness in the spacing should be corrected in order to provide proper airflow around the surface of the dome.

Summary:

- Reduce airflow leakage. Plug the cable slot gap. Check and correct leakage between sunshields and the ventilator plastic housing. Replace sun shield if necessary. Inspect entire ventilator for possible routes of airflow leakage, and perform corrective action to reduce leakage.
- Reduce airflow restrictions. Clean the intake side of the fan filter at intervals frequent enough to avoid any noticeable airflow output reduction. Confirm that the spacing between the bottom edge of the ventilator and the mounting plate is a minimum of 1 centimeter.
- Perform flow checks during each site inspection and confirm that there is not a noticeable output flow reduction. Investigate and correct any reductions in ventilator output airflow rate.
- Record entries of inspection and maintenance activities.

Additional Comments: This addendum is provided as a consolidated guide that addresses radiometer ventilator maintenance activities and correction of possible airflow leakage and/or reduction, and is not intended to address all inspection and maintenance activities that are necessary during station visits. Portions of the document provided by Chuck Long, "ARM Radiometer Ventilator Issues: An Appeal for Diligence and Improvement" have been referred to as part of preparing this addendum.

As of late 2013, the transition to DC fans having a higher flow rate than the original style AC fans provided by Eppley Laboratories is being performed as part of ECO-00991, "Radiometer Ventilation Improvements". As part of the ECO, a recommendation for a selected DC fan will be provided by the SIRS/SKYRAD/GNDRAD mentor for the ARM procurement process. Additionally, information for the procurement of associated equipment including power supplies and modified tracker mounting plates is being developed for deployment at SIRS, SKYRAD, and GNDRAD sites. The modified tracker plates are planned to have holes beneath each ventilator position for access to ventilator fan filters.


ARM
CLIMATE RESEARCH FACILITY

www.arm.gov


U.S. DEPARTMENT OF
ENERGY
Office of Science